J. DIFFERENTIAL GEOMETRY
Vol. **44** (1996) 595-633

BUBBLE TREE CONVERGENCE FOR HARMONIC MAPS

THOMAS H. PARKER

Abstract

Let Σ be a compact Riemann surface. Any sequence $f_n : \Sigma \to M$ of harmonic maps with bounded energy has a "bubble tree limit" consisting of a harmonic map $f_0 : \Sigma \to M$ and a tree of bubbles $f_k : S^2 \to M$. We give a precise construction of this bubble tree and show that the limit preserves energy and homotopy class, and that the images of the f_n converge pointwise. We then give explicit counterexamples showing that bubble tree convergence fails (i) for harmonic maps f_n when the conformal structure of Σ varies with n, and (ii) when the conformal structure is fixed and $\{f_n\}$ is a Palais-Smale sequence for the harmonic map energy.

Consider a sequence of harmonic maps $f_n : \Sigma \to M$ from a compact Riemann surface (Σ, h) to a compact Riemannian manifold (M, g) with bounded energy

$$E(f_n) = \frac{1}{2}\int_\Sigma |df_n|^2 \leq E_0. \tag{0.1}$$

Such a sequence has a well-known "Sacks-Uhlenbeck" limit consisting of a harmonic map $f_0 : \Sigma \to M$ and some "bubbles" — harmonic maps $S^2 \to M$ obtained by a renormalization process. In fact, by following the procedure introduced in [12], one can modify the Sacks-Uhlenbeck renormalization and iterate, obtaining bubbles on bubbles. The set of all bubble maps then forms a "bubble tree" ([12]). One would like to know in precisely what sense the sequence $\{f_n\}$ converges to this bubble tree. The major issue is the appearance of "necks" joining one bubble to the next.

Received August 29, 1994, and, in revised form, August 14, 1996.

Our main result (Theorem 2.2) is a precise Bubble Tree Convergence Theorem for harmonic maps. It asserts that a subsequence of the f_n in (0.1) decomposes (in the sense explained in §1) into sequences $f_{n,I}$ that converge in $L^{1,2} \cap C^0$ to the maps in the bubble tree. This includes two strong convergence statements. The first is that there is no energy loss in the limit, a fact previously shown by Jost [10]. The second is that the image of the limit is connected, that is, in the limit *there are no necks*. As a consequence, the limit preserves homology and homotopy (Corollary 2.3), and the images $f_n(\Sigma)$ converge pointwise to the image of the bubble tree map.

The bubble tree is constructed in §1 using the procedure of [12]. The construction is elementary and requires only the basic facts about harmonic maps stated in Proposition 1.1. It is also quite general: it applies to other conformally invariant semilinear equations for which the corresponding basic facts hold, such as pseudo-holomorphic maps and Yang-Mills fields.

The general analysis of §1 reduces the proof of Theorem 2.2 to showing that the energy and length of the necks vanish as $n \to \infty$. We give two proofs of these facts. In §2 we simplify and extend Jost's proof using techniques from harmonic map theory. The proof is §3 is very different: we view the necks as paths in loop space and prove the required estimates using O.D.E. methods. From this viewpoint one sees how the necks are "trying to become longer and longer geodesics" — a phenomenon ruled out by the hypotheses of Theorem 2.2, but which appears explicitly in the examples of the subsequent sections. At the end of §3 we use this approach to give a new proof of the Removable Singularities Theorem for harmonic maps.

In the final two sections we study two closely related situations where explicit counterexamples show that no bubble tree convergence theorem is possible. These examples illustrate just how subtle and delicate are the issues of energy loss and pointwise convergence on the necks.

To prove existence results for harmonic maps one would like a bubble tree convergence theorem that applies to sequences of maps that are not harmonic, but are becoming harmonic in some sense. In this context it is perhaps most natural to consider Palais-Smale sequences for the $L^{1,2}$ gradient of the energy (0.1). Yet in §4 we construct examples which dash all hope for a bubble tree convergence theorem for Palais-Smale sequences. The first is a Palais-Smale sequence of maps $S^2 \to S^2$ that approaches a degree-1 harmonic map and a degree -1 harmonic bubble map, but which loses energy in the limit. The second, more elaborate

example, is a Palais-Smale sequence that does not converge pointwise or in $L^{1,2}$ on any open set.

In the final section we consider sequences of harmonic maps from a Riemann surface (Σ, h_n) where the metric h_n is allowed to vary. If the corresponding complex structure j_n stays in a compact region in the moduli space of Σ, then the Bubble Tree Convergence Theorem 2.2 still applies (after reparameterizing the f_n). But if $\{j_n\}$ eventually leaves each compact region, then bubble tree convergence can fail. We illustrate this by constructing a specific sequence of harmonic maps $f_n : (T^2, h_n) \to S^2 \times S^1$ which fails to converge pointwise or in $L^{1,2}$ on any open set. Nevertheless, a renormalization scheme (different from the one of §1) produces a limit consisting of bubbles joined by necks. Again, there is energy loss and the necks fail to converge.

There are other approaches to existence in which one has better control on convergence than for Palais-Smale sequences. Sacks and Uhlenbeck [16] find p-harmonic maps for $p > 2$, then take a sequence with $p \to 2$. From their results one easily sees that the bubble tree construction of §1 holds for such sequences. Similarly, for the heat flow for harmonic maps Struwe [15] has a partial bubble tree convergence theorem, and Jost [10] describes an approach using the Perron method. These approaches are interesting and useful. It is clear that in each necks necessarily arise, and the issues of energy loss and C^0 convergence on the necks should be settled in these cases.

The problems raised in this paper have stimulated much recent work, and further progress on the above 'neck issues' has been made by Ding-Tian [5], Qing-Tian [13], and Chen-Tian [3].

1. The bubble tree construction

Fix a compact Riemann surface (Σ, h) and a compact Riemannian manifold (M, g). In the first three sections we will consider a sequence of harmonic maps

$$f_n : \Sigma \to M$$

with bounded energy as in (0.1). In this section we describe the "bubble tree limit" introduced in [12]. This is an inductive procedure that generalizes the Sacks-Uhlenbeck renormaliation procedure by identifying bubbles on bubbles. The construction described here is a slightly reordered version of the one in [12]. The reordering clarifies the role of the "scale size" and, more importantly, the role of the necks connecting

the bubbles. These necks are the central focus of this paper.

The basic building blocks for the bubble tree construction are the following four analytic facts about harmonic maps proved in [16].

Proposition 1.1 *There are positive constants C_1 and ϵ_0, depending only on (Σ, h) and (M, g) such that*

(a) (Sup Estimate) If $f : \Sigma \to M$ is harmonic and $D(2r)$ is a geodesic disk of radius $2r$ with energy $E(2r) = \frac{1}{2}\int_{D(2r)} |df|^2 \leq \epsilon_0$, then

$$\sup_{D(r)} |df|^2 \;\leq\; C_1 r^{-2} E(2r). \tag{1.1}$$

(b) (Uniform Convergence) If $\{f_n\}$ is a sequence of harmonic maps from a disk $D(2r)$ with $E(2r) < \epsilon_0$ for all n, then there is a subsequence that converges in C^1.

(c) (Energy Gap) Any non-trivial harmonic map $f : S^2 \to M$ has energy $E(f) \geq \epsilon_0$.

(d) (Removable Singularities) Any smooth finite-energy harmonic map from a punctured disk $D - \{0\}$ to M extends to a smooth harmonic map on D.

Combining these facts with a simple covering argument gives the following fundamental convergence result of Sacks and Uhlenbeck. To clarify the exposition the proofs of the technical Lemmas 1.2–1.6 have been relegated to the appendix.

Lemma 1.2 *Let $\{h_n\}$ be a sequence of metrics on Σ converging in C^2 to h, and $\{f_n\}$ a sequence of h_n-harmonic maps $\Sigma \to M$ with $E(f_n) \leq E_0$. Then there is a subsequence of $\{f_n\}$, a finite set of "bubble points" $\{x_1, ..., x_k\} \in \Sigma$, and an h-harmonic map $f_\infty : \Sigma \to M$ such that:*

(a) $f_n \to f_\infty$ in C^1 uniformly on compact sets in $\Sigma - \{x_1, ..., x_k\}$,

(b) the energy densities $e(f_n) = \frac{1}{2}|df_n|^2\, dv_{h_n}$ converge as measures to $e(f_\infty)$ plus a sum of point measures with mass $m_i \geq \epsilon_0$:

$$e(f_n) \to e(f_\infty) + \sum_{i=1}^{k} m_i\, \delta(x_i). \tag{1.2}$$

The construction involves six steps. The first step depends on a "renormalization constant" C_R which we are free to make smaller if needed; for now we require only that

$$C_R < \epsilon_0/2. \tag{1.3}$$

We will focus attention on one bubble point x_i, writing x_i and m_i as simply x and m. To simplify notation we adopt the convention of immediately renaming subsequences, so a subsequence of $\{f_n\}$ is still denoted $\{f_n\}$. Numbered constants, such as C_1 above, depend only on the geometry of Σ and M and on the fixed energy bound E_0.

Fix a disk $D(x, 4\rho_0)$ that contains no other bubble points and choose a sequence $\epsilon_n \to 0$ by letting $\epsilon_n \leq \min\{\rho_0, 1/n\}$ be the largest number with

$$\int_{D(x,2\epsilon_n)} e(f_\infty) \;\leq\; \frac{m}{16n^2}. \tag{1.4}$$

Step 1 (Pullback). Pullback by the exponential map, identifying f_n with $\exp_x^* f_n$ and $D(x, 2\epsilon_n)$ with the disk $D_n = D(0, 2\epsilon_n)$ in $T_x\Sigma$. The pullback measure $e(f_n)$ on D_n determines a center of mass $c_n = (c_n^1, c_n^2)$ with coordinates

$$c_n^\alpha \;=\; \frac{\int_{D_n} x^\alpha \, e(f_n)}{\int_{D_n} e(f_n)} \tag{1.5}$$

and a scale size λ_n by

(1.6)

$$\lambda_n = \text{smallest } \lambda \text{ such that } \int_{D(c_n,\epsilon_n)-D(c_n,\lambda)} e(f_n) \geq C_R,$$

where C_R is the renormalization constant (1.3).

Lemma 1.3 *After passing to a subsequence we have* $|c_n| \leq \epsilon_n/2n^2$, $\lambda_n \leq \epsilon_n/n^2$, *and there is a constant* C_3 *such that* $f_n(\partial D_n)$ *lies in the ball* $B(f_\infty(x), C_3/n)$ *in* M.

Step 2 (Renormalization). Renormalize the f_n by

1. centerizing using the translation $T_n(z) = z + c_n$,
2. rescaling by $\Lambda_n(z) = \lambda_n z$,
3. compactifying by letting $S = S_x$ be the unit 2-sphere in the fiber at x of the bundle $T_x\Sigma \oplus \mathbb{R}$; this comes with a stereographic projection $\sigma : S \to T_x\Sigma$ that takes the north pole $p^+ = (0, 0, 1) \in S$ to the origin, the south pole p^- to infinity, and the equator to the unit circle.

Then consider the composition $R_n = T_n \circ \Lambda_n \circ \sigma$ on the domain $S_n = R_n^{-1} D(0, 2\epsilon_n)$ in S and define the *renormalized maps* as the pullbacks

$$\tilde{f}_n = R_n^* f_n : S_n \to M. \tag{1.7}$$

Lemma 1.3 and the definitions of c_n and λ_n imply that the domains S_n exhaust $S - \{p^-\}$ as $n \to \infty$, and the conformal invariance of the energy means that $E(\tilde{f}_n) \leq E_0$ for all n.

Lemma 1.4 *The $\tilde{f}_n$ are harmonic with respect to metrics that converge uniformly in C^2 to the standard metric g_S on compact sets in $S_x - \{p\}$. The measures $e(\tilde{f}_n)$ have center of mass on the z-axis and satisfy*

$$\lim_{n\to\infty} \int_{S_n} e(\tilde{f}_n) = m \quad \text{and} \quad \lim_{n\to\infty} \int_{S_n^-} e(\tilde{f}_n) = C_R \tag{1.8}$$

where S_n^- is the part of S_n in the southern hemisphere.

We next find a convergent subsequence of $\{\tilde{f}_n\}$. Choose a sequence K_k of compact sets that exhaust $S - \{p^-\}$. For $k = 1, 2 \ldots$ successively apply Proposition 1.2 to the sequence $\{\tilde{f}_n\}$ on K_k, and then take the diagonal subsequence. This yields a subsequence of $\{\tilde{f}_n\}$ that converges in C^1 on $S - \{y_1, \cdots y_l, p^-\}$ to a smooth harmonic map $\tilde{f}_\infty : S \to M$, with

$$e(\tilde{f}_n) \to e(\tilde{f}_\infty) + \sum_{j=1}^{l} m_j \, \delta(y_j) + \tau(x)\delta(p^-), \tag{1.9}$$

where $m_j \geq \epsilon_0$. By Lemma 1.4 and (1.9) the center of mass of the measure $e(\tilde{f}_\infty) + \sum m_j \, \delta(y_j)$ lies on the z-axis of S. We can also assume (see appendix) that the boundaries of the domains $B_n = \sigma^{-1} D(0, n)$ satisfy

$$\tilde{f}_n(\partial B_n) \subset B(\tilde{f}_\infty(p^-), C_4/n). \tag{1.10}$$

Step 3 (Iteration). The above renormalization procedure associates to each bubble point x a sequence of harmonic maps $S_x \to M$ which converge to a harmonic map $\tilde{f}_\infty : S_x \to M$ in C^1 on $S_x - \{y_1, \ldots, y_{l(x)}, p^-\}$.

Lemma 1.5 *(a) Each secondary bubble point y_j lies in the northern hemisphere of S.*

(b) If $E(\tilde{f}_\infty) < \epsilon_0$, then $\tilde{f}_\infty$ is a map to a single point and either (i) there are $l \geq 2$ secondary bubble points, or (ii) $l = 1$ and $\tau(x) = C_R$.

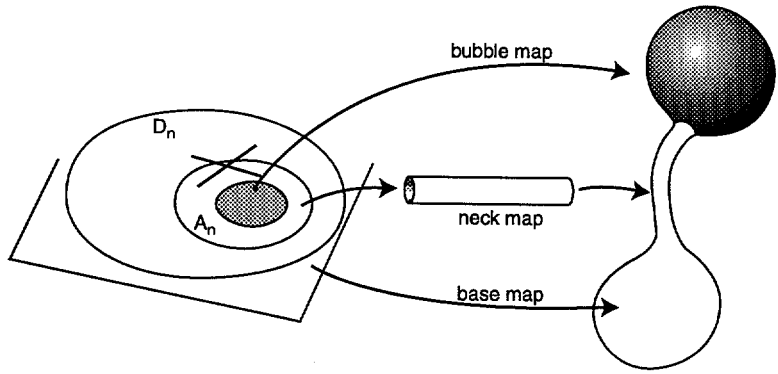

FIGURE 1

We can now repeat the renormalization around each y_j and iterate, obtaining bubbles on bubbles. Lemma 1.5b and the inequality $C_R \leq \epsilon_0/2 < m_j$ show that each iteration reduces the energy by at least C_R. Hence the process terminates after at most E_0/C_R iterations. The result is a finite tree of bubbles. Before describing this tree, we go back and modify the above procedure to keep careful track of what is happening near the south pole.

Step 4 (Extended Maps). Inside the domain $D(0, 2\epsilon_n)$ of f_n we identify three nested domains: the disks $D_n = D(c_n, \epsilon_n)$, the smaller disks $D'_n = D(c_n, n\lambda_n)$ and the annuli A_n between them (Figure 1). Doing this at each bubble point, then restricting and extending, yields three sets of maps, as follows (Figure 1).

Base Maps. Restricting f_n gives a map

$$f_n : \Sigma - \bigcup \exp_{x_i} D(c_{n,i}, \epsilon_{n,i}) \to M, \tag{1.11}$$

which, near each bubble point x, is defined outside the loop $\partial D'_n$. By Lemma 1.3 the image of this loop lies in the ball $B(f_\infty(x), C_3/n)$. Extend f_n over D_n by coning off the image:

$$\overline{f}(r, \theta) = \frac{r}{\epsilon_n} f(\epsilon_n, \theta), \tag{1.12}$$

where (r, θ) are polar coordinates around x in Σ, and the multiplication on the right is done in geodesic coordinates on $B(f_\infty(x), C_3/n)$. Doing this at each bubble point yields the *base maps*

$$\overline{f}_n : \Sigma \to M.$$

Bubble Maps. Restricting f_n to the inside disk $D(c_n, n\lambda_n) \subset T_x\Sigma$ and renormalizing give maps $R_n^* f_n : \sigma^{-1}D(0,n) \to M$; this agrees with $\tilde{f}_n$ on its domain. Using (1.10) we can again extend this to S_x by coning over the south pole. This procedure yields

$$\overline{Rf}_{n,x} : S_x \to M. \tag{1.13}$$

Neck Maps. Finally, restricting f_n to the intermediate annular region in $T_x\Sigma$ gives *neck maps*

$$f_n|_{A_n} : A_n = D(c_n, \epsilon_n) - D(c_n, n\lambda_n) \to M. \tag{1.14}$$

The base maps converge to f_∞. The maps $\tilde{f}_n$ of step 2, however, are now decomposed into the bubble maps, which converge nicely on S_x to $\tilde{f}_\infty$, and the neck maps, which are pushed into the south pole as $n \to \infty$ and account for the term $\tau(x)\delta(p^-)$ in (1.9). Specifically, after passing to a subsequence we have:

Lemma 1.6 *(a)* $\overline{f}_n \to f_\infty$ *in* $L^{1,2} \cap C^0$ *on* Σ,

(b) $\overline{Rf}_n \to \tilde{f}_\infty$ *in* $L^{1,2} \cap C^0$ *on compact sets in* $S_x - \{y_1, \cdots, y_l\}$, *and*

(c) $\tau(x) = \limsup_n E(\phi_n|_{A_n})$ *and*

$$E(f_n) \longrightarrow E(f_\infty) + \sum_{\{x_i\}} \left[\tau(x_i) + \lim_{n\to\infty} E(\tilde{f}_{n,x_i})\right]. \tag{1.15}$$

Step 5 (Renormalized Neck Maps). The domain of the neck maps (1.14) is a "no-man's land" between the base and the bubbles. On Σ, this domain shrinks into x as $n \to \infty$, while on S the renomalized domain $R_n^{-1}A_n$ shrinks into the pole p^-. Thus the neck map is a piece of the original map f_n that is not part of the base map nor the bubble map. It must be treated separately.

It is natural to renormalize the neck maps to make them maps from a cylinder. For this we write $f_n(r,\theta)$ in polar coordinates centered on c_n and consider

$$\phi_n : [0, T_n] \times S^1 \to M \text{ by } \phi_n(t,\theta) = f_n(\epsilon_n e^{-t}, \theta). \tag{1.16}$$

Note that the image of ϕ_n is the union of the loops $\gamma_{n,t} = \phi_n(t,\cdot) \subset M$ for $1 \le t \le T_n$; each has an energy

$$P_n(t) = \int_0^{2\pi} |\partial_\theta \gamma_{n,t}|^2 \, d\theta. \tag{1.17}$$

Lemma 1.7 *The neck maps (1.16) are harmonic with respect to metrics of the form* $dt^2 + \eta_n d\theta^2$ *with* $T_n \to \infty$ *and* $\eta_n \to 1$ *in* C^2 *as* $n \to \infty$, *and satisfy*

$$\sup e(\phi_n) \le C_1 C_R. \tag{1.18}$$

Moreover, for $0 \le t \le T_n$,

$$\text{length}^2\, \gamma_{n,t} \le 2\pi P_n(t) \le 2\pi C_1 C_R, \tag{1.19}$$

and at the ends

$$\text{length}^2\, \gamma_{n,0} \le 2\pi P_n(0) \le \tfrac{C_{10}}{n^2} \qquad \textit{and}$$

$$\text{length}^2\, \gamma_{n,1} \le 2\pi P_n(1) \le \tfrac{C_{10}}{n^2}.$$

Now redefine C_R to insure that the number $C_1 C_R$ is small, say $2\pi C_1 C_R < \min\{1/100, \frac{1}{2}\delta_M\}$ where δ_M is the injectivity radius of M. Then (1.19) and (1.7) show that the image of each neck map is a thin tube in M whose boundary curves are squeezed as $n \to \infty$; in fact from Lemma 1.3 and (1.10)

(1.20)
$$\gamma_{n,0} \subset B\left(f(x), \frac{C_3}{n}\right), \ \gamma_{n,T_n} \subset B\left(\tilde{f}_x(p^-), \frac{C_4}{n}\right).$$

Remark. The inner and outer radii of the neck domain A_n are somewhat arbitrary. But for any choice the ends are still squeezed as in (1.20). In fact, ϕ_n uniformly squeezes each finite region $[0, L]$ into neighborhoods of $f(x)$, and finite regions $[T_n - L, T_n]$ into neighborhoods of $\tilde{f}_\infty(p^-)$.

Step 6 (The Bubble Tower). The result of steps 1–5 is a finite tree of bubbles whose vertices are harmonic maps and the edges are bubble points. The tree is constructed from the sequence $\{f_n\}$ as follows: The $\{f_n\}$ converge to $f_\infty : \Sigma \to M$ on $\Sigma - \{x_1, \cdots, x_k\}$. The base vertex of the tree is the map f_∞, which we relabel f_0. For each x_i

the renormalization process gives a sequence $\{\phi_{n,x_i}\}$ of neck maps and a sequence $\{\overline{Rf}_n\}$ of bubble maps converging to a harmonic map $f_i : S^2_{x_i} \to M$. The pairs (x_i, ϕ_{n,x_i}) label edges eminating from the base vertex. The edge (x_i, ϕ_{n,x_i}) terminates in the vertex f_i which, in turn, is the source of new edges $\{x_{ij}\}$, and so on.

Intrinsically, the x_{ij} are points in $S\Sigma = S(T\Sigma \oplus \mathbb{R})$. Compactifiying the vertical tangent space of $S\Sigma \to \Sigma$ gives an S^2-bundle $S^2\Sigma$ over $S\Sigma$; this is where the third level of bubble points lie. Iterating yields a tower of S^2 fibrations $\cdots \to S^k\Sigma \to \cdots \to S\Sigma \to \Sigma$.

Definition. A *bubble domain* at level k is a fiber $S \cong S^2$ of $S^k\Sigma \to S^{k-1}\Sigma$. A *bubble tower* is a finite union T of bubble domains which form a tower, i.e., such that the projection of $T \cap S^k\Sigma$ lies in $T \cap S^{k-1}\Sigma$.

Given a sequence of harmonic maps, the iterated renormalization procedure singles out a bubble domain tower $T = \Sigma \cup \bigcup S_I$ and sequences of (extended) base maps $f_{n,0} = \overline{f}_n : \Sigma \to M$ and bubble maps $f_{n,I} = \overline{Rf}_{n,i_1\ldots i_k} : S_I \to M$. Together these form a sequence of *bubble tower maps* $\{f_{n,I}\} : T \to M$. By Lemma 1.6 these converge in $L^{1,2} \cap C^0$ to a limit $\{f_I\} : T \to M$.

An example of a bubble tree is shown in Figure 2. The bubble tower is at the left, the image is in the center, and the corresponding bubble tree diagram is at the right. The connecting tubes in the center picture are the images of the neck maps ϕ_{n,x_i}; these are part of the image of the original maps f_n, but are not part of the image of the bubble tower maps. Note that some bubbles may be maps to a single point; we call these *ghost bubbles*. This example includes instances of the two types of ghost bubbles described in Lemma 1.5.

Each vertex f_I of the tree has a homology class $[f_I]$ and an energy $E(f_I)$. Since the neck maps carry no homology (their images are thin tubes) we have $[f_n] = [\overline{f}_n] + \sum_{x_i}[\overline{Rf}_n]$ at each level of the bubble tree. Iterating this and (1.15) shows that the bubble tree limit preserves energy and homology in the sense that

$$E(f_n) \to E(f_\infty) \; + \; \sum [E(f_{k,x}) + \tau(x)]\,, \tag{1.21}$$

and if each f_n represents the same homology class α then

$$\alpha \; = \; [f_n] \; = \; \sum [f_I] \tag{1.22}$$

(both sums are over all bubble points x at all levels in the tree).

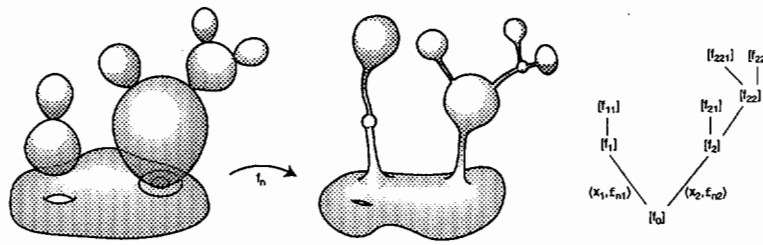

FIGURE 2

Thus far, the bubble tree construction is very general. The entire procedure requires only a conformally invariant equation with the properties of Proposition 1.1. Indeed, it was originally developed for pseudo-holomorphic maps ([12]); it also applies without change to constant mean curvature maps and the α-harmonic maps of [16], and with minor changes to Yang-Mills fields ([6]). For alternative renormalization schemes in various contexts see [1], [10], and [17]. In the next two sections we use properties special to harmonic maps to prove one last fact crucial about the bubble tree limit.

2. The bubble tree convergence theorem

The bubble tree construction of §1 associates to each bubble point x a sequence of neck maps $\phi_n : [0, T_n] \times S^1 \to M$ whose images are thin tubes in M. Using these, we can associate to x two numerical quantities:

$$\begin{cases} \text{energy loss} \quad \tau(x) = \limsup_n E(\phi_{n,x}) \\ \text{neck length} \quad \nu(x) = \limsup_n \sup_{p,q \in [0,T_n] \times S^1} \operatorname{dist}(\phi_n(p), \phi_n(q)). \end{cases}$$

In this section we will prove that both these numbers vanish.

Lemma 2.1 *At each bubble point x we have $\tau(x) = 0$ and $\nu(x) = 0$.*

Lemma 2.1 completes our analysis of the bubble tree, and, with the results of §1, immediately gives our main convergence theorem.

Theorem 2.2 (Bubble Tree Convergence for Harmonic Maps). *Let $\{f_n\} : \Sigma \to M$ be a sequence of harmonic maps from a fixed Riemann surface (Σ, h) to a compact Riemannian manifold (M, g)*

with $E(f_n) \leq E_0$. Then there is a subsequence $\{f_n\}$ and a bubble tower domain T so that the renormalized maps

$$\{f_{n,I}\} : T \to M$$

converge in $L^{1,2} \cap C^0$ to a smooth harmonic bubble tree map $\{f_I\} : T \to M$. Moreover,

(a) (No energy loss) $E(f_n)$ converges to $\sum E(f_I)$, and

(b) (Zero distance bubbling) At each bubble point x_J (at any level in the tree), the images of the base map f_I and the bubble map f_J meet at $f_I(x_J) = f_J(p^-)$.

Consequently the image of the limit $\{f_I\} : T \to M$ is connected, and the images of the original maps $f_n : \Sigma \to M$ converge pointwise to this image $\{f_I\}$.

Thus the image of the limit map appears like the first picture in Figure 2 instead of the middle picture. *The limiting image has no necks.*

Remark. Theorem 2.2 is exactly the result proved in [12] for J-holomorphic maps. For harmonic maps the "no energy loss" statement was previously proved by Jost ([10]). The argument below uses aspects of both these proofs. It simplifies Jost's argument and includes the zero distance bubbling statement and the precise statement of the convergence of the images.

Zero distance bubbling implies that the bubble tree limit preserves homotopy. Each map $f_n : \Sigma \to M$ represents a class $[f_n]$ in the set $[\Sigma, M]$ of free homotopy classes. A bubble tree map $f : T = \Sigma \cup \bigcup S_I \to M$ also has a class $[f] \in [\Sigma, M]$ obtained by succesively adding the bubble maps to the class $[f_0]$ of the base map as follows. For each bubble point x_J of f_I, choose a path γ from the image point $f_I(x_J)$ to $f_J(p^-)$, the image of the basepoint of the bubble domain S_J. Then form the connected sum by mapping an annulus around x_J to the boundary of a tubular neighborhood of γ and the interior of this annulus to M by stereographic projection and the bubble map — this reverses the bubbling procedure. In general the choice of γ is well-defined only up to $\pi_1(M)$. However, by Theorem 2.2b there is a canonical choice, and with that choice we have the following homotopy statement.

Corollary 2.3 *If each f_n represents the same homotopy class in $[\Sigma, M]$, then*

$$\alpha = [f_n] = \sum [f_I] \tag{2.1}$$

(sum over all vertices of the bubble tree). If $\Sigma = S^2$, then this statement is true in $\pi_2(M)$. The corresponding homology statement (1.22) also holds.

The proof of Lemma 2.1 is based on the observation that a harmonic map can be "suspended" to give a conformal harmonic map. This trick was first used by Schoen [14] to prove a regularity result; his method was simplified by Grüter [7] and used in the present context by Jost [10].

To describe the suspension process, we consider a harmonic map $f : D \to M$ from a disk D with energy $E(f)$ and Hopf differential

$$\psi_f \, dz^2 \;=\; \left[\, |f_x|^2 - |f_y|^2 \;-\; 2i \,\langle f_x, f_y\rangle \,\right] \, dz^2. \tag{2.2}$$

Recall that ψ is holomorphic, and vanishes if and only if f is conformal. The suspension F of f is defined by finding the unique solution to

$$\overline{\partial}\xi = 0, \qquad \partial\xi = -\frac{1}{4}\psi_f, \qquad \xi|_{\partial D} = 0 \tag{2.3}$$

and setting

$$F \;=\; (f, \overline{z} + \xi) \;:\; D \to M \times \mathbb{C}.$$

Then F is harmonic *and conformal*, since its Hopf differential $\psi_F = \psi_f + 4\partial(\overline{z} + \xi)\partial(z + \overline{\xi}) = \psi_f + 4\partial\xi\partial z$ vanishes. Moreover, since ψ is holomorphic with L^1 norm bounded by $2E(f)$, we have the pointwise bounds

$$|\psi| \le 4c_1 E(f) \tag{2.4}$$

and $\frac{1}{2}|d(\overline{z} + \xi|^2 = 1 + |\psi|^2/16 \le 1 + c_1^2 E(f)$. Hence the energy of F on any subdomain $A \subset D$ satisfies

$$\begin{aligned} \int_A e(F) \;&=\; \int_A e(f) \;+ \left(1 + \frac{1}{16}|\psi_f|^2\right) \\ &\le \; \int_A e(f) \;+\; \text{Area}(A)\left[1 + c_1^2 E^2(f)\right], \end{aligned} \tag{2.5}$$

and for the circle $S_r \subset D$ of radius r

$$\begin{aligned} \text{length}(F(S_r)) \;&\le\; \int_0^{2\pi} |\partial_\theta f| + |\partial_\theta(\overline{z} + \xi| \, d\theta \\ &\le\; \text{length}(f(S_r)) + 2r\left(1 + c_1^2 E(f)\right). \end{aligned} \tag{2.6}$$

The advantage of *conformal* harmonic maps is that their images are minimal surfaces. We can then use the following standard measure-theoretic facts about minimal surfaces.

Lemma 2.4 *Let (M, g) be a closed Riemannian manifold and let Σ be a minimal surface in $(M \times \mathbb{R}^2, g + dx^2 + dy^2)$. Then there are constants $c_M, \epsilon_M > 0$ such that if* $\text{Area}(\Sigma) < \epsilon_M$, *then*

(a) (Isoperimetric Inequality) $\text{Area}(\Sigma) \leq c_M \text{ length}^2(\partial\Sigma)$, *and*

(b) (Monotonicity) for any ball $B(p, \delta)$ around $p \in \Sigma$ that contains no part of $\partial\Sigma$

$$\text{Area}(\Sigma \cap B(p, \delta)) \geq \frac{\delta^2}{4c_M^2}. \tag{2.7}$$

Proof. Statement (a) follows from the isoperimetric inequality of Hoffman and Spruck [9]. Monotonicity is an easy consequence: by (a) the function $A(r) = \text{Area}(\Sigma \cap B(p, r))$ satisfies $\sqrt{A(r)} \leq c_M A'(r)$; integrating from 0 to δ gives (2.7). q.e.d.

The proof of Lemma 2.1 is now quite simple.

Proof of Lemma 2.1. Apply the bubble tree construction of §1 with $C_R = \frac{1}{2}\min\{\epsilon_0, \epsilon_M\}$, where these are the constants of Proposition 1.1 and Lemma 2.4. Then, starting with the sequence $\{f_n\} : D(c_n, \epsilon_n) \to M$ around a bubble point, form the suspended maps and restrict to the collar domain A_n of (1.14), obtaining conformal harmonic maps $F_n : A_n \to M \times \mathbb{C}$. Let $\Sigma_n = F_n(A_n)$ be the image surface. Since the energy of a conformal map is the area of the image, (2.5) shows that

$$\text{Area}(\Sigma_n) \;=\; E(F_n) \;\leq\; E(f_n) + c_2\epsilon_n^2 \;\leq\; C_R + c_2/n^2,$$

so $\text{Area}(\Sigma_n) \leq \epsilon_M$ for all large n. Moreover, as $n \to \infty$ the lengths of the boundary curves $\partial\Sigma$ go to 0 by (2.6) and (1.7). Applying the isoperimetric inequality,

$$E(f_n) \;\leq\; E(F_n) \;=\; \text{Area}(\Sigma_n) \leq\; c_M \,\text{length}^2(\partial\Sigma_n) \to 0, \tag{2.8}$$

and hence $\tau(x) = 0$.

The statement $\nu(x) = 0$ now follows from monotonicity. Fix $\delta > 0$. Since the lengths of the curves $\partial\Sigma_n$ go to 0, there are points $P, Q \in M \times \mathbb{C}$ such that $\partial\Sigma_n \subset B(P, \delta) \cup B(Q, \delta)$ for all large n. By (2.8) we also have $\text{Area}(\Sigma_n) \leq \delta^2/8c_M^2$ for all large n. If, for some large n, there is a point $R \in \Sigma_n$ not in $B(P, 2\delta) \cup B(Q, 2\delta)$, then monotonicity gives the contradictory statement $\delta^2 \leq 4c_M^2 \,\text{Area}(\Sigma_n \cap B(R, \delta)) \leq \delta^2/2$. Therefore $\Sigma_n \subset B(P, 2\delta) \cup B(Q, 2\delta)$, and, since Σ_n is connected, $\Sigma_n \subset B(P, 4\delta)$ for all large n. Hence $\nu(x) = 0$. q.e.d.

3. Path space

In this section we give a second proof of Lemma 2.1. This proof is direct and elementary, and uses no any special techniques from harmonic map theory. The viewpoint introduced in the proof is an important prelude to the examples in §4 and §5.

From Lemma 1.7 the neck maps are a sequence of maps $\phi_n : [0, T_n] \times S^1 \to M$ that are harmonic for metrics $dt^2 + \eta_n d\theta^2$ (with $\eta_n \to 0$ in C^2) and have energy

$$E(\phi_n) \;=\; \frac{1}{2}\int_0^{T_n}\int_0^{2\pi} |\partial_t \phi_n|^2 + \eta^{-1}|\partial_\theta \phi_n|^2 \,\sqrt{\eta}\, d\theta dt \;\le\; C_R.$$

Equivalently, ϕ_n associates to each t a loop $\gamma_t(\theta) = \phi(t, \theta)$ in M and thus defines a path

$$[0, T_n] \to \mathcal{L}_M$$

in the free loop space $\mathcal{L}_M = L^{1,2}(S^1, M)$. From this viewpoint, $E(\phi)$ can be thought of as a Lagrangian

$$L(\phi) \;=\; \frac{1}{2}\int_0^{T_n} \|\dot\phi\|^2 + P(t)\; dt, \tag{3.1}$$

which is the sum of kinetic and potential energy terms

$$\|\dot\phi\|^2 \;=\; \int_0^{2\pi} |\partial_t \phi|^2 \,\sqrt{\eta}\, d\theta, \;\; P(t) \;=\; \int_0^{2\pi} |\partial_\theta \phi|^2 \,\frac{d\theta}{\sqrt{\eta}}. \tag{3.2}$$

This Lagrangian describes the motion of a point particle moving in loop space in the potential $-P$. By Lemma 1.7 the trajectories corresponding to the neck maps lie near the set $\mathcal{M} \subset \mathcal{L}_M$ where $-P$ assumes its maximum; this is the submanifold $\mathcal{M} \cong M$ of point maps along which $L(\phi)$ reduces to the geodesic energy. One can visualize two types of trajectories in $\mathcal{L}_M$ as in Figure 3. Trajectory A rises, follows a geodesic along the "ridge" $\mathcal{M}$, and then falls; the corresponding surface in M is the long neck of Figure 3b. Trajectory B rises and falls with little motion along $\mathcal{M}$, corresponding to the small neck of Figure 3c. We will show that the neck map trajectories are of type B.

The estimates below use two facts about the neck maps ϕ_n:

(a) ϕ_n extends to a finite-energy harmonic map $[0, \infty) \times S^1 \to M$ (by (1.16), noting that the neck maps f_n in (1.14) extends over the disk), and

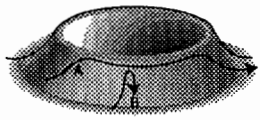

FIGURE 3A

FIGURE 3B

FIGURE 3C

(b) $E(\phi_n) \leq C_R$, where we can choose C_R smaller if needed.

Our first lemma shows that property (a) implies that $E(\phi_n)$ can be calculated from the function $P(t)$. This is equivalent to Lemma 3.5 in [16]; the proof is transparent in the present context. Our second lemma derives an inequality for $P(t)$ using methods familiar from the theory of geodesics. A simple comparison argument then proves Lemma 2.1.

Lemma 3.1 *If $\phi : [0,T] \times S^1 \to M$ is harmonic and extends as in (a) above, then*

$$E = \int_0^T P(t)\, dt. \tag{3.3}$$

Proof. The Hamiltonian corresponding to the Lagrangian (3.1), namely

$$H(t) = \frac{1}{2}\left[\, \|\dot{\phi}_t\|^2 - P(t) \,\right], \tag{3.4}$$

is a constant of motion. Since ϕ has finite energy $\int_0^\infty H(t)\, dt \leq E(\phi) < \infty$, so $H = 0$. Hence the integral (3.1) reduces to (3.3). q.e.d.

Lemma 3.2 *If C_R is sufficiently small, then for each ϕ_n with n large*

$$P''(t) > \frac{1}{4}P(t) \geq 0. \tag{3.5}$$

Proof. Set $X = \phi_*(\partial/\partial_\theta)$, $T = \phi_*(\partial/\partial_t)$, and $\overline{d\theta} = \eta^{-1/2} d\theta$. Then $P(t)$ is the integral of $|X|^2 \overline{d\theta}$, and $P'(t)$ is the sum of the first variation in the T direction and the t derivative of the metric:

$$P'(t) = \int_0^{2\pi} 2\langle X, \nabla_X T\rangle - \xi\, |X|^2\, \overline{d\theta},$$

where $\xi = \frac{1}{2}\eta^{-1}\dot{\eta}$. Differentiating again and computing the second variation in the usual way (cf. [2]), we obtain

$$P''(t) = \int_0^{2\pi} 2|\nabla_T X|^2 + 2\langle R(T,X)T, X\rangle + 2\langle \nabla_X \nabla_T T, X\rangle - 4\xi\langle X, \nabla_T X\rangle + (\xi^2 - \dot{\xi})|X|^2 \, \overline{d\theta},$$

where ∇ and R are respectively the covariant derivative and the Riemannian curvature of M. Now integrate the term involving $\nabla_X \nabla_T T$ by parts, subsitute in the harmonic map equation

$$\nabla_T T = -\eta^{-1}\nabla_X X - \xi T + \zeta X, \qquad \zeta = \frac{1}{2}\eta^{-2}\partial_\theta \eta,$$

and estimate, using $|\langle X, \nabla_T X\rangle| \le |X|^2 + |\nabla_T X|^2$ and the similar inequalities for $\langle X, \nabla_X X\rangle$ and $\langle X, T\rangle$. Since $\eta \to 1$ in C^2 as $n \to \infty$, we obtain

$$\begin{aligned} P''(t) \ge & \int_0^{2\pi} 2\left(|\nabla_X T|^2 + \eta^{-1}\,|\nabla_X X|^2\right) \overline{d\theta} \\ & - 2\|R\|_\infty \|T\|_\infty^2 \int_0^{2\pi} |X|^2 \, \overline{d\theta} \\ & - c(n) \int_0^{2\pi} |\nabla_T X|^2 + |\nabla_X X|^2 + |X|^2 + |T|^2 \, \overline{d\theta} \end{aligned} \tag{3.6}$$

with $c(n) \to 0$. But $|R|$ is bounded, $|T|^2 \le |d\phi|^2 \le C_1 C_R$ by (1.18), and the integral of $\eta|T|^2 \, \overline{d\theta}$ is the integral of $|X|^2 \, \overline{d\theta}$ since the Hamiltonian (3.4) vanishes. Thus for large n

$$P''(t) \ge \int_0^{2\pi} |\nabla_X X|^2 - c_1 C_R P(t). \tag{3.7}$$

By (1.19) and the choice of C_R made after Lemma 1.7, the image curve $\gamma_t = \phi(t, \cdot)$ lies in a coordinate chart of radius $R = \sqrt{C_1 C_R}$. In this chart the metric is uniformly equivalent to the euclidean metric and the Christoffel symbols satisfy $|\Gamma| \le c_2 R \le c_2\sqrt{C_1 C_R}$. Moreover, for any $\mathbb{R}^n$-valued function γ on S^1 Fourier expansion shows that

$$\int_0^{2\pi} \left|\partial_\theta \gamma\right|^2 \le \int_0^{2\pi} \left|\partial_\theta^2 \gamma\right|^2.$$

Hence

$$\int_0^{2\pi} |X|^2 \leq \int_0^{2\pi} |\partial_\theta X|^2 = \int_0^{2\pi} |\nabla_X X - \Gamma(X,X)|^2$$

$$\leq 2\int_0^{2\pi} |\nabla_X X|^2 + 2\|\Gamma\|_\infty^2 \|X\|_\infty^2 \int_0^{2\pi} |X|^2. \tag{3.8}$$

Using the above bound on Γ and (1.18), $|\Gamma||X| \leq |\Gamma||d\phi| \leq c_2 C_1 C_R$. Hence for C_R small the last term in (3.8) can be absorbed on the left, giving

$$\frac{3}{4}\int_0^{2\pi} |X|^2 \leq 2\int_0^{2\pi} |\nabla_X X|^2. \tag{3.9}$$

The norms in (3.9) are with respect to the euclidean metrics on Σ and M in normal coordinates; for large n and small C_R these can be replaced by the metric norms after increasing the constant slightly. Thus (3.9) yields

$$P(t) \leq 3\int_0^{2\pi} |\nabla_X X|^2, \tag{3.10}$$

and the lemma follows by combining (3.7) and (3.10) and taking $C_R < 1/12c_1$.

Proposition 3.3 *There is a constant c_3 such that for all large n*
(a) $E(\phi_n) \leq c_3/n^2$, *and*
(b) dist $(\phi_n(p), \phi_n(q)) \leq c_3/n$ *for all points* $p, q \in [0, T_n] \times S^1$.

Proof. Fix n. By Lemma 3.2, $P(t)$ satisfies $P'' \geq \frac{1}{4}P$ with initial conditions $P(0) = \epsilon_1$ and $P(T_n) = \epsilon_2$. Let $f(t)$ be the solution of

$$f'' = \frac{1}{4}f, \qquad f(0) = \epsilon_1, \qquad f(T_n) = \epsilon_2.$$

Then $P(t) \leq f(t)$ by the maximum principle. Explicitly, $f(t) = Ae^{t/2} + Be^{-t/2}$ with

$$A = \frac{1}{1-\alpha^2}(\epsilon_1 - \alpha\epsilon_2), \quad B = \frac{\alpha}{1-\alpha^2}(\epsilon_2 - \alpha\epsilon_1), \tag{3.11}$$

and $\alpha = e^{T_n/2}$. Hence by Lemma 3.1 we have

$$E = \int_0^{T_n} P(t)\, dt \leq \int_0^{T_n} Ae^{t/2} + Be^{-t/2}\, dt = 2(\alpha - 1)\left[A + \frac{B}{\alpha}\right].$$

Subsitututing for A and B, simplifying, and using (1.7) yield

$$E \leq 2\left(\frac{\alpha-1}{\alpha+1}\right)(\epsilon_1+\epsilon_2) \leq 2\left[P(0)+P(T_n)\right] \leq \frac{c_3}{n^2}.$$

To bound the length of the image we compute the length of the curve $\phi(t,\theta)$ for $0 \leq t \leq T_n$ for each fixed θ, and average over θ. This average length $\mathcal{L}$ satisfies

$$\mathcal{L} = \frac{1}{2\pi}\int_0^{T_n}\int_0^{2\pi}\left|\frac{d\phi}{dt}\right| d\theta dt \leq \frac{\sqrt{2\pi}}{2\pi}\int_0^{T_n}\left(\int_0^{2\pi}|T|^2\, d\theta\right)^{1/2} dt.$$

Noting that (3.4) vanishes and that η is uniformly close to 1, we have

$$\frac{1}{2}\left(\int_0^{2\pi}|T|^2\, d\theta\right)^{1/2} \leq \sqrt{P(t)} \leq \sqrt{f(t)} \leq |A|^{1/2}e^{t/4} + |B|^{1/2}e^{-t/4}.$$

Integration gives

$$\sqrt{2\pi}\,\mathcal{L} \leq 8(\sqrt{\alpha}-1)\left(|A|^{1/2} + |\frac{B}{\alpha}|^{1/2}\right).$$

Using the definitions of α, A, and B, and simplifying, we get

(3.12)
$$\sqrt{2\pi}\,\mathcal{L} \leq 16\sqrt{\epsilon_1+\epsilon_2}\left(\frac{\sqrt{\alpha}-1}{\sqrt{\alpha^2-1}}\right) \leq 16\sqrt{P(0)+P(T_n)}.$$

Finally, note that $P(t)$ has no strict interior maximum on $[0,T_n]$ since $P'' \geq 0$ by (3.5). Thus the loop $\gamma_t = \phi_n(t,\cdot)$ has

$$\text{length}^2\,(\gamma_t) \leq 2\pi P(t) \leq 2\pi\left[P(0)+P(T_n)\right]. \tag{3.13}$$

For points $p = (t_1,\theta_1), q = (t_2,\theta_2)$ in $[0,T_n]\times S^1$, (3.12), (3.13) and (1.7) yield

$$\text{dist}\,(\phi_n(p),\phi_n(q)) \leq \text{length}\,(\gamma_{t_1}) + \mathcal{L} + \text{length}\,(\gamma_{t_2}) \leq c_3/n.$$

q.e.d.

Proposition 3.3 implies Lemma 2.1, thus giving a second route to Theorem 2.2. In fact, Proposition 3.3 is a sharper result: it shows that the length of the neck *measured along the image* goes to 0, while Lemma 2.1 shows only that the image lies balls with radii going to 0.

Finally, the argument of this section gives a new proof of the Removablity Singularities Theorem (Proposition 1.1d above and Theorem 3.6 in [16]).

Proof of Removablity Singularities. Integration by parts with a cut-off function shows that f is weakly harmonic (cf. [12, Lemma 3.5]). It then suffices to establish an energy growth rate

$$\int_{D(0,r)} e(f) \leq Cr^{\alpha} \tag{3.14}$$

for $r \leq r_0$ and some $\alpha > 0$ (by [11, Theorem 3.5.2]; this implies that f is Hölder continuous, and hence is smooth by standard bootstrap arguments). The map $\phi : \mathbb{R} \times S^1 \to M$ defined by $f(r,\theta) = \phi(e^{-t},\theta)$ is harmonic with finite energy, and by Lemma 3.1, (3.14) is equivalent to

$$\begin{aligned} E(t,\infty) &= \int_t^{\infty} \int_0^{2\pi} e(f) \\ &= \int_t^{\infty} P(s)\, ds \leq Ce^{-\alpha t} \end{aligned} \tag{3.15}$$

for $t \geq t_0$. Choose t_0 such that $E(t_0,\infty)$ is small enough that Lemma 3.2 applies, and choose a sequence $t_i \to \infty$ with $P(t_i) \to 0$. Applying the comparison argument of Proposition 3.3 on $[t_0,t_i]$ shows that $P(s) \leq A_i e^{s/2} + B_i e^{-s/2}$; solving for A_i and B_i and letting $t_i \to \infty$ reduce this to $P(s) \leq P(t_0)\exp[(t_0-s)/2]$. Integrating over $[t,\infty)$ then gives (3.15) with $\alpha = 1/2$. q.e.d.

The above proof simplifies further because we can assume (by making an initial conformal change of metric) that the metric is locally euclidean.

4. Palais-Smale sequences

This section presents examples that show that energy loss can occur for Palais-Smale sequences for the energy function

$$E(f) = \frac{1}{2}\int_{\Sigma} |df|^2$$

with respect to the natural $L^{1,2}$ metric. Of course, there are numerous technical problems arising because $L^{1,2}$ is the "borderline" norm. However, the recent regularity result of Helein [8] (that weakly harmonic $L^{1,2}$

maps are smooth) has renewed interest in proving a bubble convergence theorem for Palais-Smale sequences of $L^{1,2}$ maps. The examples below show that this cannot be done: a general Palais-Smale sequence simply does not have enough regularity to have good convergence properties.

Remark. Because the $L^{1,2}$ norm is borderline, the space of maps $L^{1,2}(\Sigma, M)$ is not a manifold. Hence we must be careful about the definition of Palais-Smale sequence. On a Hilbert manifold a sequence $\{f_n\}$ is Palais-Smale if $E(f_n) < E_0$ and $\| \operatorname{grad} E(f_n)\| \to 0$. This latter condition is equivalent to $dE_{f_n} \to 0$ as a functional on the tangent space. We will use this definition, interpreting the $L^{1,2}$ "tangent space" to be the $L^{1,2}$ completion of the smooth variational vector fields. Thus we say that $\{f_n\}$ is Palais-Smale if $E(f_n) < E_0$ and

$$|dE_{f_n}(X)| \leq c_n \|X\|_{1,2} \qquad \text{with} \qquad c_n \to 0. \tag{4.1}$$

Our examples are based on the following elementary observation. Let $\gamma : [0, T] \to M$ be a geodesic parameterized proportion to arclength. Then the map

$$f : [0, T] \times S^1 \to M$$

by $f(t, \theta) = \gamma(t)$ is harmonic — since f is independent of θ, the harmonic map equation

$$\partial_t^2 f^i + \partial_\theta^2 f^i = \Gamma^i_{jk} \left(\partial_t f^j \partial_t f^k + \partial_\theta f^j \partial_\theta f^k \right)$$

reduces to the geodesic equation. The energy of this harmonic map depends on the parameterization: if the image geodesic has length L, then

$$E(f) = \frac{1}{2} \int_0^T \int_0^{2\pi} |\dot{\gamma}|^2 \, dt = \frac{\pi L^2}{T}. \tag{4.2}$$

Thus, even if L is fixed, we can choose T to make the energy $E(f)$ equal to any given number.

Using this observation we can construct a Palais-Smale sequence $\Phi_n : S^2 \to M$ by the following general procedure. First choose two harmonic maps, a base map $f : S^2 \to M$, a bubble map $h : S^2 \to M$, and a closed geodesic γ in M that intersects the images of f and h. Fix an arclength-proportional parameterization of γ with $p = \gamma(0) \in \operatorname{im}(f)$ and $q = \gamma(a + bn) \in \operatorname{im}(g)$ for each $n \in \mathbb{Z}$. After a rotation we can assume that there is a point $x \in S^2$ with $f(x) = p$ and $h(x) = q$. Then

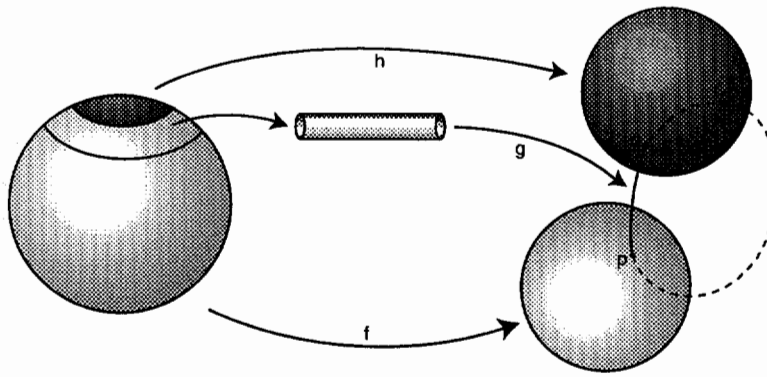

FIGURE 4

choose disks $D(x,\delta_n) \subset D(x,\epsilon_n)$ and define maps $\Phi_n : S^2 \to M$ that agree with f outside $D(x,\epsilon_n)$, that take $D(x,\delta_n)$ onto most of the image of h (by conformally rescaling h), and take the annulus between these disks first to a cylinder $[0,T] \times S^1$, then to the geodesic γ starting at p, wrapping around n times, and ending at q (see Figure 4). When ϵ_n and δ_n are choosen appropriately, these maps Φ_n give a Palais-Smale sequence that loses energy in the neck.

This construction can already be carried out when the target manifold is the 2-sphere. Later in this section we will fill in the details to prove the following specific result.

Proposition 4.1 *For each $\alpha > 0$ there is a Palais-Smale sequence $\{\Phi_n\}$ of smooth maps $S^2 \to S^2$ that converges pointwise on $S^2 - \{x\}$ to a degree-1 harmonic map f, and after renormalization at x converges to a degree -1 harmonic map h, and satisfies*

$$\lim_{n\to\infty} E(\Phi_n) = E(f) + E(h) + \alpha. \tag{4.3}$$

The maps Φ_n represent the same homotopy class, but their images have no pointwise limit.

The same construction reveals a more fundamental impediment to a bubble tree convergence theorem. Recall that by Lemma 1.1b a sequence of harmonic maps cannot bubble unless a certain threshhold of energy concentrates at a point. It was this fact that allowed us, in the proof of Lemma 1.2, to identify the bubble points and show that each bubble carries a certain minimal amount of energy. Our second example shows

that Lemma 1.1b fails for Palais-Smale sequences: there is no such energy threshold, and energy loss can occur on a dense set.

Proposition 4.2 *For each $\alpha > 0$ and $x \in S^2$ there is a Palais-Smale sequence $\{\Phi_n\}$ of smooth maps $S^2 \to S^2$ that converges pointwise on $S^2 - \{x\}$ to a harmonic map f with*

$$\lim_{n\to\infty} E(\Phi_n) = E(f) + \alpha. \tag{4.4}$$

More generally, given any countable set of points $\{x_i\} \subset S^2$ and positive numbers $\{\alpha_i\}$ with $\sum \alpha_i < \infty$, there is a Palais-Smale sequence that loses energy α_i at each x_i. If $\{x_i\}$ is dense, this sequence fails to converge in $L^{1,2}$ or C^0 on any open set in the domain.

The remainder of this section is devoted to the proofs of Propositions 4.1 and 4.2. We first construct the sequence $\{\Phi_n\}$ of Proposition 4.1, and then verify the Palais-Smale property, and modify the construction to prove Proposition 4.2.

Fix a number $\alpha > 0$. For each $n > 0$ set

$$\delta_n = e^{-\sqrt{n}} \qquad \text{and} \qquad \epsilon_n = \frac{1}{n} e^{-n^2/\alpha},$$

and consider $\mathbb{R}^2$ as the overlapping union of the disk $D(0, \epsilon_n/\delta_n^2)$ and the annuli $A(\epsilon_n, \frac{1}{n})$ and $A(\delta_n^2/n, \infty)$. We will construct maps $\phi_n : \mathbb{R}^2 \to S^2$ by defining maps f_n, g_n, h_n on these domains and patching them together on the overlap annuli

$$A_n = A\left(\frac{\delta_n^2}{n}, \frac{\delta_n}{n}\right), \qquad B_n = A\left(\frac{\epsilon_n}{\delta_n}, \frac{\epsilon_n}{\delta_n^2}\right).$$

(i) Let $f_n : A(\delta_n^2/n, \infty) \to S^2$ be the restriction of the stereographic projection f from $\mathbb{R}^2$ to the unit sphere $S^2 \subset \mathbb{R}^3$; this is the conformal harmonic map given explicitly by

$$f(x,y) = \left(\frac{2x}{1+r^2}, \frac{2y}{1+r^2}, \frac{1-r^2}{1+r^2}\right), \qquad r^2 = x^2 + y^2.$$

(ii) Define $g_n : A(\epsilon_n, \frac{1}{n}) \to [0, n^2/\alpha] \times S^1 \to S^2$ by composing the conformal map $(r,\theta) \mapsto (-\log(nr), \theta)$ with an arclength-proportional parameterization of a geodesic that winds around the sphere n times:

$$g_n(r,\theta) = \left(-\sin\left[\frac{2\pi\alpha}{n}\log(nr)\right], 0, \cos\left[\frac{2\pi\alpha}{n}\log(nr)\right]\right).$$

Then as in (4.2) each g_n is harmonic with energy

$$E(g_n) = 4\pi^3\alpha. \tag{4.5}$$

(iii) Define $h_n : D(0, \epsilon_n/\delta_n^2) \to S^2$ by inverting and rescaling the stereographic projection f; thus h_n is the conformal harmonic map

$$h_n(x,y) = f(\frac{\epsilon_n^2 x}{r^2}, \frac{\epsilon_n^2 y}{r^2}).$$

We next patch these maps together over A_n and B_n using "log cutoff functions" β_n and η_n defined as follows. Choose smooth functions $\overline{\beta}$ and $\overline{\eta}$ with

$$\overline{\beta}(t) = \begin{cases} 1 & \text{for } t \le \sqrt{n}, \\ 0 & \text{for } t \ge 2\sqrt{n}, \end{cases} \qquad \overline{\eta}(t) = \begin{cases} 1 & \text{for } t \le n^2/\alpha - 2\sqrt{n}, \\ 0 & \text{for } t \ge n^2/\alpha - \sqrt{n}, \end{cases}$$

and with $0 \le \overline{\beta}, \overline{\eta} \le 1$, $|\overline{\beta}'| \le 2/\sqrt{n}$, and $|\overline{\eta}'| \le 2/\sqrt{n}$ pointwise. Then the cutoff functions

$$\beta_n(r,\theta) = \overline{\beta}(-\log(nr)) \qquad \text{and} \qquad \eta_n(r,\theta) = \overline{\eta}(-\log(nr))$$

satisfy

$$\int_{A_n} |d\beta_n|^2 \le \frac{8\pi}{\sqrt{n}}, \qquad \int_{B_n} |d\eta_n|^2 \le \frac{8\pi}{\sqrt{n}}. \tag{4.6}$$

Define the patched-together map by

$$\phi_n = \beta_n f + (1-\beta_n)\eta_n g_n + (1-\eta_n)h_n. \tag{4.7}$$

Outside the regions A_n and B_n only one term in (4.7) is non-zero. For $z \in A_n \cup B_n$, $f_n(z), g_n(z)$, and $h_n(z)$ lie near the north pole p of S^2, and (4.7) means the sum in stereographic coordinates around p. More specifically, one checks that

(4.8)
$$\begin{aligned} &f(A_n) \subset B(p, 2/n), \quad f(A_n \cup B_n) \subset B(p, 4\pi\alpha/\sqrt{n}), \\ &h(B_n) \subset B(p, 2/n). \end{aligned}$$

Finally, define $\Phi_n : S^2 \to S^2$ by composing stereographic projection $f^{-1} : S^2 \to \mathbb{R}^2$ with ϕ_n. These Φ_n represent the same homotopy class (since $\pi_1(S^2) = 1$) and their images have no pointwise limit (Φ_n wraps n times around S^2). Hence Proposition 4.1 is proved by the following lemma.

Lemma 4.3 *$\{\Phi_n = \phi_n \circ f^{-1}\}$ is a Palais-Smale sequence satisfying (4.1).*

Proof. Only one term of (4.7) is non-zero outside $A_n \cup B_n$, so

$$E(\phi_n) = \frac{1}{2}\left[\int_{A(\delta/n,\infty)} |df|^2 + \int_{A(\epsilon/\delta^2,\delta^2/n)} |dg_n|^2 + \int_{D(0,\epsilon/\delta)} |dh_n|^2 + \int_{A_n\cup B_n} |d\phi_n|^2\right].$$

Since the energy is conformally invariant, we have $E(\Phi_n) = E(\phi_n)$ and $E(h_n) = E(f)$ over corresponding domains. Calculating the energy of g_n as in (4.5) and taking the limit give

(4.9)
$$\lim_{n\to\infty} E(\Phi_n) = 2E(f) + 4\pi^3\alpha + \frac{1}{2}\lim_{n\to\infty}\int_{A_n\cup B_n} |d\phi_n|^2.$$

Differentiating (4.7) and taking the L^2 norm, we obtain

$$\int_{A_n\cup B_n} |d\phi_n|^2 \le 3\int_{A_n} |df|^2 + |dg_n|^2 + |d\beta_n(f-g_n)|^2 + 3\int_{B_n} |dg_n|^2 + |dh_n|^2 + |d\eta_n(g_n - h_n)|^2.$$

From the defintions of f, g_n and h_n one calculates that

$$|df|^2 = 8/(1+r^2)^2 \le 8, \quad |dg_n| = 2\pi\alpha/nr, \quad |dh_n| = 4\epsilon^2/(r^2+\epsilon^4).$$

From (4.8) we know $|f-g_n| \le \frac{4\pi}{\sqrt{n}}(\alpha+1)$ on A_n and $|g_n - h_n| \le \frac{4\pi}{\sqrt{n}}(\alpha+1)$ on B_n, and also, in consequence of (4.6),

(4.10)
$$\int_{A_n\cup B_n} |d\phi_n|^2 \le c_1(\alpha+1)^2 n^{-3/2}.$$

Combining this with (4.9) gives (4.3) and shows that the energies $E(\Phi_n)$ are uniformly bounded.

It remains to verify (4.1), where X is a smooth vector field tangent to $S^2 \subset \mathbb{R}^3$ along the image of Φ_n. Thus we have $X \cdot \Phi_n = 0$ pointwise, and

$$dE_{\Phi_n} = (d^*d\Phi_n)^T = d^*d\Phi_n - |d\Phi_n|^2\Phi_n,$$

where d^*d is the Laplacian on S^2, and T denotes this projection onto the tangent space to $S^2 \subset \mathbb{R}^3$. But X is already tangent, and dE_{Φ_n} vanishes everywhere except on the domains $\mathcal{A}_n$ and $\mathcal{B}_n$ in S^2 which correspond to A_n and B_n under stereographic projection, so

$$dE_{\Phi_n}(X) = \int_{S^2} \langle X, d^*d\Phi_n \rangle = \int_{\mathcal{A}_n \cup \mathcal{B}_n} \langle X, d^*d\Phi_n \rangle \, . \tag{4.11}$$

Now introduce log cutoff functions $\zeta_n(r,\theta) = \overline{\zeta}(-\log(nr))$, where $\overline{\zeta}$ has support on $[0, 3\sqrt{n}] \cup [n^2/\alpha - 3\sqrt{n}, n^2/\alpha]$, is equal to 1 on $[\sqrt{n}, 2\sqrt{n}]$ and $[n^2/\alpha - 2\sqrt{n}, n^2/\alpha - \sqrt{n}]$, and satisfies $0 \le \overline{\zeta} \le 1$ and $|\overline{\zeta}'| \le 2/\sqrt{n}$ pointwise. Then ζ_n is identically 1 on $A_n \cup B_n$ and has support on the larger annuli $A'_n = A(\delta_n^3/n, 1/n)$ and $B'_n = A(\epsilon_n, \epsilon_n/\delta_n^3)$.

Expanding the annuli A_n and B_n in this way makes little difference; in particular one can check that, as in (4.6) and (4.10),

$$\begin{aligned} \int_{A'_n \cup B'_n} |d\zeta|^2 &\le \frac{32\pi}{\sqrt{n}}, \\ \int_{A'_n \cup B'_n} |d\phi_n|^2 &\le c_2(\alpha+1)^2 n^{-3/2}. \end{aligned} \tag{4.12}$$

We can then replace X by $\zeta_n X$ in the middle term of (4.12) and integrate by parts,

$$|dE_{\Phi_n}(X)| = \int_{S^2} \langle \zeta_n X, d^*d\Phi_n \rangle = \int_{A'_n \cup B'_n} \langle dX, \zeta_n d\Phi_n \rangle + \langle d\zeta_n, X \cdot d\Phi_n \rangle.$$

Differentiating the condition $X \cdot \Phi_n = 0$ gives $X \cdot d\Phi_n = -dX \cdot \Phi_n$, with $|\Phi_n| \le 1$ pointwise. Hence by Hölder's inequality, the conformal invariance of the L^2 norm, and (4.13) we obtain

$$\begin{aligned} |dE_{\Phi_n}(X)| &\le (\|\zeta_n d\Phi_n\|_2 + \|d\zeta_n\|_2) \, \|dX\|_2 \\ &\le \left(\|d\phi_n\|_{2, A'_n \cup B'_n} + \|d\zeta_n\|_{2, A'_n \cup B'_n}\right) \, \|dX\|_{2, S^2} \\ &\le c_3(\alpha+1)^2 n^{-1/2} \, \|X\|_{1,2}, \end{aligned}$$

which is the Palais-Smale condition (4.1). q.e.d.

Proof of Propostion 4.2. Simply replace the maps h_n in (4.7) by the point map $h_n(z) = p$ where p is the north pole of S^2. The resulting maps Φ_n are then degree-one maps $S^2 \to S^2$ with a "tail": a small

neighborhood of one point is taken to a geodesic that winds n times around the image S^2. The proof of Lemma 4.3 (without change) shows that this sequence is Palais-Smale, and (4.4) replaces (4.3).

For each n this construction modifies the map $f : S^2 \to S^2$ in a disk $D(x, 1/n)$ (by adding a tail of energy α) to produce a map Φ_n. Write $\Phi_n = T(x, \alpha)f$, where $T(x, \alpha)$ denotes this operation of adding a tail.

Now fix a countable dense set of distinct points $\{x_i\}$ in S^2 and numbers $\alpha_i > 0$ with $\sum \alpha_i < \infty$. For each $k = 1, 2 \ldots$ there is an M_k such that the disks $D(x_i, 1/M_k)$, $i = 1, \ldots, k$, are disjoint, and then

$$\Phi_{n,k} = T(x_k, \alpha_k) \cdots T(x_2, \alpha_2) T(x_1, \alpha_1) f$$

is well-defined for all $n \geq M_k$. As in (4.9) and (4.10) we have

(4.13)

$$E(\Phi_{n,k}) \;\leq\; E(f) + 4\pi^3 \sum^{k} \alpha_i + c_1 n^{-3/2} \sum^{k} (\alpha_i + 1)^2.$$

Thus the energies $E(\Phi_{n,k})$ are bounded uniformly once we pass to a subsequence with $n \geq k$. The remainder of the proof of Lemma 4.3 shows that

$$|dE_{\Phi_n}(X)| \;\leq\; c_3 n^{-1/2} \sum^{k} (\alpha_i + 1)^2 \; \|X\|_{1,2} \;\leq\; c_4(\alpha)\, k\, n^{-1/2} \; \|X\|_{1,2}.$$

Choose a subsequence $\{\Phi_k = \Phi_{n_k,k}\}$ inductively by setting $n_{k+1} = \max\{n_k + 1, M_k, k^4\}$. This sequence has bounded energy and satisfies $|dE_{\Phi_n}(X)| \leq c_4 k^{-1} \|X\|_{1,2}$, so is Palais-Smale. But it clearly fails to converge in $L^{1,2}$ or C^0 on any open set. q.e.d.

5. Varying the conformal structure

Thus far we have considered maps from a Riemann surface Σ with a fixed Riemannian metric h. In this section we allow the metric to vary, and ask how sequences of harmonic maps $f_n : (\Sigma, h_n) \to M$ can degenerate. Of course, the hypotheses of the Bubble Tree Convergence Theorem 2.2 are conformally invariant, so it is only the conformal classes of the metrics $\{h_n\}$ that are relevent. The hypotheses are also invariant under reparameterizations so, modulo reparameterization, only the complex structures j_n associated to the h_n are relevent. In particular, if these complex structures range over a compact region in moduli space,

then $\{f_n\}$ has a subsequence whose images converge pointwise to the connected image of a bubble tree map. On the other hand, we will show by an explicit example that if the conformal classes are unbounded in moduli space, then the bubble tree convergence procedure can break down completely.

Proposition 5.1 *There is a sequence $\{h_n\}$ of conformal structures on the torus T^2 and a sequence of harmonic maps $\phi_n : (T^2, h_n) \to M = S^2 \times S^1$ with $E(f_n) \leq E_0$ such that every subsequence fails to converge in C^1 on every open set $U \subset T^2$.*

In the example the images, as sets in M, do exhibit some regularity — they look like "necklaces" as in Figure 5. Later in this section we give a renormalization procedure that makes sense of the limit as the image of a collection of "bead maps" $S^2 \to M$. This renormalization is completely different from the one of §1. Moreover, energy is lost in the limit.

To produce the example, we look for harmonic maps from $\mathbb{R} \times S^1$ into $S^2 \times \mathbb{R}$, where S^2 is the unit sphere. Using coordinates $(\vec{u}, v)$ on $S^2 \times \mathbb{R} \subset \mathbb{R}^3 \times \mathbb{R}$, the second fundamental form is

$$h\left((\vec{u}, v), (\vec{u}, v)\right) = |\vec{u}|^2 (\nu, 0),$$

where ν is the unit normal. We seek a harmonic map f of the form

$$f(t, \theta) = \left(r(t) \cos\theta,\, r(t) \sin\theta,\, z(t),\, w(t) \right)$$

with $r^2 + z^2 = 1$. Fixing the metric $dt^2 + d\theta^2$ on $\mathbb{R} \times S^1$, one finds that

$$h(\nabla f, \nabla f) = \left(r^2 + \dot{r}^2 + \dot{z}^2\right) \left(r\cos\theta,\, r\sin\theta,\, z,\, 0 \right).$$

Then f satisfies the harmonic map equation $\Delta f = -h(\nabla f, \nabla f)$ if and only if

$$\begin{aligned} &(a)\quad \ddot{z}(t) &&= z(z^2 - 1) - \tfrac{z\dot{z}^2}{1-z^2}, \\ &(b)\quad \ddot{r}(t) &&= r(1 - r^2) - \tfrac{r\dot{r}^2}{1-r^2}, \\ &(c)\quad \ddot{w}(t) &&= 0. \end{aligned} \tag{5.1}$$

It is easy to check that if z satisfies (5.1a), then $r = \sqrt{1 - z^2}$ satisfies (5.1b). Equation (5.1a) can be rewritten as

$$\frac{d}{dt}\left(\frac{\dot{z}^2}{1 - z^2} + z^2 \right) = 0,$$

and hence

$$\dot{z}^2 = (1-z^2)(c-z^2) \tag{5.2}$$

for some constant c. We are looking for non-trivial solutions with $|z| \leq 1$ for all t, so (5.2) implies that $c > 0$; we will rewrite this constant as $c = 1/k^2$ for some $k > 0$. The solution of (5.2) is then the elliptic integral

$$t(z) + t_0 = k \int_0^z \frac{d\zeta}{\sqrt{(1-\zeta^2)(1-k^2\zeta^2)}}.$$

Inverting this gives the solutions of (5.2) in terms of Jacobi elliptic functions (cf. [4]):

$$\begin{cases} z(t) = \mathrm{sn}(\frac{t-t_0}{k}, k), \\ r(t) = \sqrt{1-z^2} = \mathrm{cn}(\frac{t-t_0}{k}, k), \\ w(t) = at + b. \end{cases}$$

Thus we get solutions depending on four parameters. Two of these — the time translation t_0 and the translation of the image b — do not affect the geometry. Setting these equal to zero, we have a 2-parameter family of harmonic maps $f_{k,a} : \mathbb{R} \times S^1 \to S^2 \times \mathbb{R}$ given by

$$f_{k,a}(t,\theta) = (\mathrm{cn}(t/k,k)\cos\theta,\ \mathrm{cn}(t/k,k)\ \sin\theta,\ \mathrm{sn}(t/k,k),\ at)\,. \tag{5.3}$$

When $k = 1$, the Jacobi functions reduce to hyperbolic trigonometric functions; in particular $\mathrm{sn}(t,1) = \tanh(t)$, and $\mathrm{cn}(t,1) = \mathrm{sech}(t)$. For $k < 1$ the functions $\mathrm{sn}(t/k,k)$ and $\mathrm{cn}(t/k,k)$ are periodic in t with period $4Kk$, where K is the complete elliptic integral

$$K = \int_0^1 \frac{d\zeta}{\sqrt{(1-\zeta^2)(1-k^2\zeta^2)}}. \tag{5.4}$$

Like the ordinary trigonometric functions they also satisfy

$$\begin{aligned} \mathrm{sn}(t+2Kl,k) &= (-1)^l \mathrm{sn}(t,k), \\ \mathrm{cn}(t+2Kl,k) &= (-1)^l \mathrm{cn}(t,k) \end{aligned} \tag{5.5}$$

for integers l. Now as k approaches 1 the period $4Kk$ becomes arbitrarily large. Thus given a positive integer p and a real number $\alpha > 0$ we can

choose an increasing sequence $k_n \to 1$ with $4K_nk_n = n^2/\alpha$ and take $k = k_n$ and $a = \alpha/np$ in (5.3). After composing with the projection $S^2 \times \mathbb{R} \to S^2 \times \mathbb{R}/\mathbb{Z}$, this gives a sequence of harmonic maps $f_n : \mathbb{R} \times S^1 \to S^2 \times S^1$ that are periodic in t with period $4K_nk_np$. Then

$$\phi_n(t) = f_n(4K_nk_npt) \tag{5.6}$$

are harmonic maps on $S^1 \times S^1$ with the metric $(4K_nk_np)^2dt^2 + d\theta^2$, and hence are also harmonic for the conformal metric

$$h_n = dt^2 + (4K_nk_np)^{-2}d\theta^2 = dt^2 + (\alpha/n^2p)^2d\theta. \tag{5.7}$$

Note that the conformal classes of these metrics $\{h_n\}$ are unbounded in the moduli space of the torus.

Lemma 5.2 *Let T_n be the torus $S^1 \times S^1$ with the metric (5.7), and let $M = S^2 \times S^1$ be the product of the unit 2-sphere and the circle of length 1. Then the functions*

$$\begin{aligned}\phi_n(t,\theta) = {} & (\mathrm{cn}(4K_npt, k_n)\cos\theta,\ \mathrm{cn}(4K_npt, k_n)\sin\theta,\\ & \mathrm{sn}(4K_npt, k_n),\ nt \pmod 1)\end{aligned} \tag{5.8}$$

give harmonic maps $\phi_n : T_n \to M$ with $E(f_n) \le E_0$ (see below).

Looking at the last component we see that $|\partial_t\phi_n| \ge n$ at each point, so the statement of Proposition 5.1 clearly holds for this sequence.

Henceforth consider the subseqence of $\{\phi_n\}$ with $n = 2pm + 1$, $m = 1, 2, 3, \ldots$. In the remainder of this section we will use a renormalization method to describe the geometry of this subsequence.

The image of ϕ_n is a "necklace" consisting of $2p$ "beads" strung together by $2p$ strings; Figure 5 depicts the case $p = 2$. The map ϕ_n is equivariant under the rotation $t \mapsto t + 1/p$, and because of (5.6) the energy density (5.12 below) is invariant under $t \mapsto t + 1/2p$. To analyze these we divide the torus into "bead domains" and "string domains". The l^{th} bead domain of ϕ_n is a thin cylinder centered on $t = l/2p$:

$$B_l = \left\{(t,\theta) : \left|t - \frac{l}{2p}\right| \le n^{-3/2}\right\},$$

and the l^{th} string domain is the cylinder between B_l and B_{l+1}:

$$S_l = \left\{(t,\theta) : \frac{l}{2p} + n^{-3/2} \le t \le \frac{l+1}{2p} - n^{-3/2}\right\}. \tag{5.9}$$

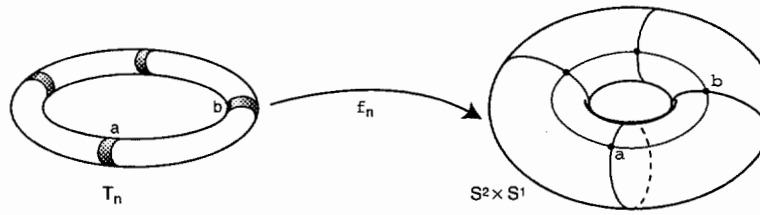

FIGURE 5. The map ϕ_n takes the four shaded annuli in T_n to approximations to the corresponding vertical spheres in $S^2 \times S^1$. It takes the neck between loops a and b into a thin tube near the geodesic that goes from α to β around the circle $\{\text{north pole}\} \times S^1$ m times, and then on to β.

Beads. Consider the restriction of ϕ_n to the bead domain B_l. Translating by $t \mapsto t + l/2p$, reversing steps (5.6) and (5.7) above, and using (5.6), this corresponds to the harmonic map

$$\left((-1)^l \mathrm{cn}(\frac{t}{k_n}, k_n)\ \cos\theta,\ (-1)^l \mathrm{cn}(\frac{t}{k_n}, k_n)\ \sin\theta,\right.$$
$$\left.(-1)^l \mathrm{sn}(\frac{t}{k_n}, k_n),\ \frac{\alpha t}{np} + \frac{l}{2p} \pmod 1\right), \tag{5.10}$$

defined on the domain $\Omega_n = [-p\sqrt{n}/\alpha, p\sqrt{n}/\alpha] \times S^1$ with metric $dt^2 + d\theta^2$. Next recall that there is a conformal map $\mu : \mathbb{R} \times S^1 \to S^2$ ("Mercator projection") given by $\mu(t,\theta) = (\mathrm{sech}\ t \cos\theta,\ \mathrm{sech}\ t \sin\theta, \tanh t)$. Pulling back by μ^{-1} gives the *renormalized bead map*

$$R^l\phi_n : (\mu^{-1})^*\phi_n\ :\ \mu(\Omega_n) \to M.$$

Lemma 5.3 *As $n \to \infty$, the renormalized bead maps $R^l\phi_n$ converge to $\phi^l_\infty = ((-1)^l\,\mathrm{Id.}, l/2p) : S^2 \to S^2 \times S^1$ uniformly on compact sets in $S^2 - \{(0,0,\pm 1)\}$.*

Proof. As $k = k_n \to 1$ we have $\mathrm{cn}(t/k, k) \to \mathrm{sech}(t)$ and $\mathrm{sn}(t/k, k) \to \tanh(t)$ uniformly on compact sets. Thus $\phi_n \to ((-1)^l\mu, l/2p)$ uniformly on Ω_N for each $N > 0$. The lemma follows because the domains $\mu(\Omega_N)$ exhaust $S^2 - \{(0,0,\pm 1)\}$ as $N \to \infty$.

Strings. On the string domains the maps ϕ_n behave very much like the necks in the examples of §4 — the images become longer and longer geodesics.

Lemma 5.4 *The image $\phi_n(S_l)$ of each string domain is a thin tube that wraps more than m times around the S^1 factor of $M = S^2 \times S^1$. As $n \to \infty$ this tube has* circumference $\to 0$ *and energy*

$$\int_{S_l} e(\phi_n) \to \frac{\pi\alpha}{2p^2}. \tag{5.11}$$

Proof. Let π be the projection $M \to S^1$. For each fixed θ the curve $\gamma(t) = \pi \circ \phi_n(t, \theta)$ has $\dot{\gamma} = n = 2pm + 1$. Integrating over the limits (5.9) shows that length$(\gamma) \cong m + 1/2p$ for large n.

Using the properties of the Jacobi elliptic functions (cf. [4]) and the metric (5.7) one finds that the energy density $e(\phi) = \frac{1}{2}h^{ij}\partial_i\phi\partial_j\phi\,\sqrt{h}\,dtd\theta$ is

$$e(\phi_n)(t) = \left[\tfrac{\alpha}{2p} + 2K_n p\left(\tfrac{1-k_n^2}{k_n^2} + 2\mathrm{cn}^2(4K_n pt, k_n)\right)\right] dtd\theta. \tag{5.12}$$

Integrating over S_l, changing variables to $\tau = 4Kkpt$, and noting that the function $\xi(t) = \mathrm{cn}^2(t/k, k)$ is $2Kk$-periodic by (5.6), we obtain

$$\int_{S_l} e(\phi_n) = 2\pi\left[\left(\frac{\alpha}{2p} + 2Kp\frac{1-k^2}{k^2}\right)\left(\frac{1}{2p} - \frac{1}{\sqrt{n}}\right) + \frac{1}{k}\int_\nu^{2Kk-\nu} \xi(\tau)\,d\tau\right],$$

where $\nu = p\sqrt{n}/\alpha$. As $n \to \infty$ we have $k_n \to 1$ and by (5.4)

$$4K(1-k^2) \le 4\sqrt{1-k^2}\int_0^1 \frac{d\zeta}{\sqrt{1-\zeta^2}} = \pi\sqrt{1-k^2} \to 0.$$

Thus, after noting that $\xi(2Kk - t/k, k) = \xi(t)$ by (5.6),

$$\int_{S_l} e(\phi_n) \to \frac{\pi\alpha}{2p^2} + \frac{4\pi}{k}\lim_{n\to\infty}\int_\nu^{Kk} \xi(\tau)\,d\tau. \tag{5.13}$$

Again using basic properties of the elliptic functions one finds that on $[0, Kk]$

$$\xi' = -\frac{2}{k}\sqrt{\xi(1-\xi)(1-k^2+k^2\xi)} \le -2\xi\sqrt{1-\xi},$$

since $k \le 1$. On the other hand, $g(\tau) = \mathrm{sech}^2\,\tau$ satisfies $g' = -2g\sqrt{1-g}$ with $\xi(0) = g(0) = 1$, $\xi'(0) = g'(0) = 0$, and $\xi''(0) < -2 = g''(0)$. It follows that on $[0, Kk]$

$$\xi(\tau) = \mathrm{cn}^2(\tau/k, k) \le \mathrm{sech}^2(\tau) \le 4e^{-2\tau}. \tag{5.14}$$

One then sees that the limit in (5.13) is zero, so (5.13) reduces to (5.11). Finally, for t in the range (5.9), we can bound the length of the loop $\phi_n(t,\theta)$ using (5.8) and (5.14), obtaining

$$\int_0^{2\pi} |\partial_\theta \phi_n| \, d\theta = 2\pi \, |\mathrm{cn}(4K_n p t, k_n)| \leq 4\pi \, \exp(-\frac{n^2 p}{\alpha} t)$$

$$\leq 4\pi \, \exp(-\frac{p\sqrt{n}}{\alpha}) \to 0.$$

q.e.d.

The total energy of ϕ_n comes from the $2p$ beads, each with energy 4π, and the $2p$ strings, each with energy (5.11). Thus

$$E(\phi_n) \to 8p\pi + \frac{\pi\alpha}{p}. \tag{5.15}$$

This gives the last statement of Lemma 5.2.

The beads in this example are different from the bubbles of §1 — energy is not concentrating at isolated points and the renormalization of step 2 of §1 does not apply. Nevertheless, Lemmas 5.3 and 5.4 do give a bubble graph (it is not a tree) that describes the limit: it has $2p$ vertices labeled by the bead maps ϕ_∞^l joined in a circle by $2p$ edges labeled by the string maps $\phi_n|_{S_l}$. These string maps are clearly part of the same general picture as the proofs of §3 and the examples of §4. But now, because the metrics are changing, the Bubble Tree Convergence Theorem 2.2 fails: *energy is lost in the strings and the images do not converge pointwise.* The energy lost – the last term in (5.15) – can be choosen to be any positive number.

6. Appendix

This appendix contains the proofs of Lemmas 1.2–1.7. These proofs are elementary but technical; they use only the facts stated in Proposition 1.1. Some of these proofs can be simplified by assuming — after an initial conformal change — that the metric is euclidean. We have avoided this to make the proofs adaptable to other contexts.

Proof of Lemma 1.2. Cover Σ by δ-balls such that the balls of half the size also cover and such that each point lies in at most 10 balls. At most $10E_0/\epsilon_0$ of these balls contain energy greater that ϵ_0; passing

to a subsequence we can assume that the centerpoints of these balls converge. Let $\Omega = \Omega(\delta)$ be the union of these limit 'high energy' balls. By Lemma 1.1b we can choose a subsequence that coverges in C^1 on $\Sigma - \Omega(\delta)$. Doing this successively with $\delta = \delta_i \to 0$ and taking the diagonal subsequence give a subsequence $\{f_n\}$ that converges in C^1 on $\Sigma - \cap_i \Omega(\delta_i)$ to a limit f_∞. Moreover, the intersection $\cap_i \Omega(\delta_i)$ consists of points $\{x_1, \ldots, x_l\}$ with $l \leq 10E_0/\epsilon_0$. Then f_∞ is smooth and harmonic on $\Sigma - \{x_1, \ldots, x_l\}$, and therefore extends to a smooth harmonic map $f_\infty : \Sigma \to M$ by Lemma 1.1d. It also follows that the energy densities converge as in (1.2). Finally, if $m_i < \epsilon_0$ for some i, then integrating (1.2) over a sufficiently small disk $D(x_i, 2r_0)$ we see that (1.1) applies, giving a uniform bound on $e(f_n)$ for all large n, so $e(f_n)$ could not be approaching a δ measure. q.e.d.

Proof of Lemma 1.3. Choose a subsequence $\{f_{n_k}\}$ inductively as follows. Given $k \geq 1$, write $D_k = D(0, 2\epsilon_k)$ as the union of $\mathcal{B}_k = D(0, \epsilon_k/8k^2)$ and the annulus $\mathcal{A}_k = D_k - \mathcal{B}_k$. By (1.2) and (1.4) there is an N_k such that for all $n \geq N_k$

$$\text{(A.1)} \qquad \begin{aligned} \frac{8k^2-1}{8k^2} m \;&\leq \int_{\mathcal{B}_k} e(f_n) \;\leq\; \frac{8k^2+1}{8k^2} m, \\ \int_{\mathcal{A}_k} e(f_n) \;&\leq \frac{m}{8k^2}. \end{aligned}$$

By Lemma 1.2 we can also assume that for $n \geq N_k$

$$\text{(A.2)} \qquad \begin{aligned} \sup_{z \in \partial D_k} \operatorname{dist}(f_n(z), f_\infty(z)) &\leq \frac{1}{k}, \\ \sup_{D_1 - \mathcal{B}_k} |e(f_n) - e(f_\infty)| &\leq 1. \end{aligned}$$

Set $n_k = \max\{N_k, 1 + n_{k-1}\}$. Starting with $n_0 = 1$, this defines a subsequence $\{f_{n_k}\}$, which we immediately rename $\{f_n\}$. Then for each n the denominator in (1.5) is at least $m(8n^2-1)/8n^2$, while

$$\int_{D_n} |x|\, e(f_n) \;\leq\; \epsilon_n/8n^2 \int_{\mathcal{B}_n} e(f_n) + 2\epsilon_n \int_{\mathcal{A}_n} e(f_n) \;\leq\; \epsilon_n m \left[\frac{24n^2+1}{64n^4}\right].$$

Hence $|c_n| \leq \epsilon_n/2n^2$. We thus have $\mathcal{B}_n \subset \mathcal{B}' = D(c_n, \epsilon_n/n^2)$, so for each n

$$\int_{D_n - \mathcal{B}'} e(f_n) \;\leq\; \int_{\mathcal{A}_n} e(f_n) \;\leq\; \frac{m}{8n^2} \;\leq\; \frac{\epsilon_0}{8n^2} \;\leq\; C_R.$$

It follows from (1.6) that $\lambda_n \leq \epsilon_n/n^2$. Finally, applying (1.1) on disks in Σ with radius equal to the injectivity radius of Σ gives

$$\sup_{\Sigma} |df_\infty|^2 \leq C_2 E_0. \tag{A.3}$$

Using this and (A.2) we have

$$\begin{aligned} \operatorname{dist}(f_\infty(x), f_n(\partial D_n)) &\leq 2\epsilon_n \sup |df_\infty| + \sup_{z\in\partial\mathcal{D}_n} \operatorname{dist}(f_n(z), f_\infty(z)) \\ &\leq \frac{C_3}{n}. \end{aligned} \tag{A.4}$$

q.e.d.

Proof of Lemma 1.4. Write the metric on $T_x\Sigma$ as $\exp_x^* g = g_0 + h$ where g_0 is the euclidean metric and $h = h_{ij}dx^i dx^j$ satisfies $|h| \leq c\epsilon_n^2$, $|\partial h| \leq c'\epsilon_n$, and $|\partial^2 h| \leq c''$ on $D(0, 2\epsilon_n)$. Recall that σ is conformal: $\sigma^* g_0 = \psi g_S$ for some function ψ. Then $\tilde{f}_n$ is harmonic for the pullback metric

$$\begin{aligned} \sigma^*\Lambda_n^* T_n^* [g_0 + h] &= \sigma^*\lambda_n^2 \left[g_0 + (\Lambda_n^* T_n^* h_{ij})dx^i dx^j\right] \\ &= \psi\lambda_n^2 \left[g_S + \psi^{-1}\sigma^*(\Lambda_n^* T_n^* h_{ij})dx^i dx^j\right], \end{aligned}$$

and hence for the conformal metric $g_S + \psi^{-1}\sigma^*(\Lambda_n^* T_n^* h_{ij})dx^i dx^j$. Because ψ and σ_* are smooth away from p^-, convergence follows by bounding the C^2 norm of $\Lambda_n^* T_n^* h_{ij}(z) = h_{ij}(\lambda_n(z + c_n))$ on its domain. But this is bounded by the sup of $|h| + |\lambda_n \partial h| + |\lambda_n^2 \partial^2 h|$ on D_n, which is less than $c'''\epsilon_n^2 \to 0$ by the above bounds and Lemma 1.3.

The energy of $\tilde{f}_n$ in S_n is the energy of f_n on D_n, which converges to m by (A.2). Similarly, the energy of $\tilde{f}_n$ in S_n^- is the energy of f_n in $D(0, \epsilon_n) - D(c_n, \lambda_n)$, which is C_R by definition (1.6), plus the energy of f_n in $D_n - D(0, \epsilon_n)$, which converges to 0 by (A.2). Finally, by definition the measures $e(T_n^* f_n)$ – and hence $e(\Lambda_n^* T_n^* f_n)$ — have center of mass at the origin, so $e(\tilde{f}_n)$ has center of mass on the z-axis. q.e.d.

The inclusion (1.10) is obtained by repeating the argument of Lemma 1.3. Specifically, as in (A.4) we can pass to a subsequence to insure that

$$\sup_{z\in B_n} \operatorname{dist}(\tilde{f}_n(z), \tilde{f}_\infty(z)) \leq \frac{1}{n}, \quad \sup_{B_n} |e(\tilde{f}_n) - e(\tilde{f}_\infty)| \leq 1. \tag{A.5}$$

As in (A.3) and (A.4) we then obtain

(A.6)
$$\sup_S |d\tilde{f}_\infty|^2 \;\leq\; C_1 E_0,\; \operatorname{dist}(\tilde{f}_\infty(p^-), \tilde{f}_n(\partial B_n)) \;\leq\; \frac{C_4}{n}.$$

Proof of Lemma 1.5. Integrating (1.9) over S_n^-, comparing with (1.8) and noting that $m_j \geq \epsilon_0 > C_R$ show that each y_j lies in the northern hemisphere.

If $E(\tilde{f}_\infty) < \epsilon_0$, then by Proposition 1.1c $\tilde{f}_\infty$ is a map to a point and $e(\tilde{f}_\infty) \equiv 0$. The limit measure $\sum m_j \delta(y_j) + \tau\delta(p^-)$ in (1.9) has center of mass on the z-axis, and by (1.8) has energy C_R in the southern hemisphere and energy $m - C_R > 0$ in the northern hemisphere. This is impossible if $l = 0$, and if $l = 1$ it implies that y_1 is the north pole and $\tau = C_R$. q.e.d.

Before proceeding we make two observations. First, from (A.2) and (A.3) we have

(A.7)
$$\sup_{D_1 - D(0,\epsilon_n/8)} e(f_n) \;\leq\; 1 + \sup e(f_\infty) \;\leq\; 1 + C_2 E_0 \;=\; C_5.$$

Similarly, (A.5) and (A.6) give

(A.8)
$$\sup_{B_n} e(\tilde{f}_n) \;\leq\; C_6.$$

Second, we can bound the energy of the cone extension (1.12) as follows. The metric on $D_n' = D(c_n, \epsilon_n)$ is uniformly equivalent to the euclidean metric, so for large n $\overline{f}_n$ satisfies

$$\begin{aligned}\int_{D_n'} e(\overline{f}_n) \;&\leq\; \int_{D_n'} |\partial_r \overline{f}_n|^2 + |r^{-1}\partial_\theta \overline{f}_n|^2 \; r dr d\theta \\ &= \int_0^{\epsilon_n}\int_0^{2\pi} \left|\frac{\overline{f}_n(\epsilon_n,\theta)}{\epsilon_n}\right|^2 + \left|\frac{1}{r}\partial_\theta f_n(\epsilon_n,\theta)\right|^2 \; r dr d\theta.\end{aligned}$$

But $|f_n(\epsilon_n,\theta)| \leq C_3/n$ by Lemma 1.3, and on the circle $\partial D_n'$ we have $|r^{-1}\partial_\theta f_n| \leq |df_n| \leq \sqrt{C_5}$ by (A.7). Thus

(A.9)
$$\int_{D_n'} e(\overline{f}_n) \;\leq\; 2\pi \left(\int_0^{\epsilon_n} r \; dr\right)\left(\frac{C_3^2}{\epsilon_n^2 n^2} + C_5\right) \;\leq\; \frac{C_7}{n^2}.$$

Using (A.6) and (A.8) we get a similar bound for the extensions (1.13).

Proof of Lemma 1.6. For notational simplicity we assume there is only one bubble point. By Lemma 1.3 the off-center disks $D_n' = D(c_n, \epsilon_n)$ in (1.11) satisfy $D(0, \epsilon_n/2) \subset \overline{D}_n \subset D_n = D(0, 2\epsilon_n)$. Hence for $n \geq k \geq 1$, (A.9) and (A.7) yield

(A.10)
$$\begin{aligned} \int_{D_k} e(\overline{f}_n) &= \int_{D_n'} e(\overline{f}_n) + \int_{D_k - D_n'} e(f_n) \\ &\leq C_8 \left(\frac{1}{n^2} + \epsilon_k^2 \right). \end{aligned}$$

Also, connecting each $z \in D_k$ by a line to the nearest point in ∂D_n and using the triangle inequality, Lemma 1.3, (1.12), and (A.7) we obtain

$$\begin{aligned} \operatorname{dist}(\overline{f}_n(D_k), f_\infty(x)) &\leq \operatorname{dist}(\overline{f}_n(D_n), f_\infty(x)) + 2\epsilon_k \sup_{D_k - D_n} |df_n| \\ &\leq \frac{C_3}{n} + 2\epsilon_k \sqrt{C_5}. \end{aligned} \tag{A.11}$$

Now fix $\delta > 0$ and choose k large enough that ϵ_k, (A.10), and (A.11) are all less that δ for all $n \geq k$. With this k, we have $f_n \to f_\infty$ in C^1 on $\Sigma - D_k$. Consequently

$$\int_\Sigma \left| e(\overline{f}_n) - e(f_\infty) \right| + \sup_{z \in \Sigma} \operatorname{dist}(\overline{f}_n(z), f_\infty(z)) \leq C_9 \delta$$

for all large n. It follows that $\overline{f}_n \to f_\infty$ in $L^{1,2} \cap C^0$ on Σ. The same argument, now using (A.8) and (1.10), shows that $\overline{Rf}_n \to f_\infty$ in $L^{1,2} \cap C^0$ on any compact set in $S - \{y_j\}$.

The partitioning done in step 3 of §1 accounts for all the energy, and the extension adds only a small amount by (A.9); hence

$$E(f_n) \longrightarrow E(f_\infty) + \lim_{n \to \infty} \sum_{\{x_i\}} \left[E(f_n|_{A_{n,i}}) + E(\overline{Rf}_{n,i}) \right].$$

Now the sets $B_k = \sigma^{-1} D(0, k)$ exhaust S as $k \to \infty$, and for $n > k$ the domain S_n of $\tilde{f}_n$ contains B_k. Thus

$$\begin{aligned} \tau &= \lim_{k \to \infty} \lim_{n \to \infty} \int_{S_n - B_k} e(\tilde{f}_n) \\ &= \lim_{k \to \infty} \lim_{n \to \infty} \left[\int_{S_n - B_n} e(\tilde{f}_n) + \int_{B_n - B_k} e(\tilde{f}_n) \right]. \end{aligned}$$

The sup bound (A.8) implies that this last integral vanishes in the limit. Since $S_n - B_n = R_n^{-1}\left[D(0, 2\epsilon_n) - D(c_n, n\lambda_n)\right]$, we have

(A.12)

$$\tau \;=\; \lim_{k\to\infty}\lim_{n\to\infty}\left[\int_{D(0,2\epsilon_n)-D(c_n,\epsilon_n)} e(f_n) + \int_{A_n} e(f_n)\right].$$

By Lemma 1.3, $D(0, 2\epsilon_n) - D(c_n, \epsilon_n)$ lies in the domain $\mathcal{A}_n$ of (A.2). Hence the first integral in (A.12) vanishes as $n \to \infty$, and after taking a subsequence the second converges to $\limsup E(\phi_n)$. q.e.d.

Proof of Lemma 1.7. In polar-normal coordinates $\exp_x^* g = dr^2 + r^2\eta(r,\theta)d\theta^2$ where $|1-\eta| \le cr^2$, $|\partial\eta| \le c'r$, and $|\partial^2\eta| \le c''$. Writing $\Phi_n(t,\theta) = (\epsilon_n e^{-t}, \theta)$, we see that $\phi_n = \Phi_n^* f_n$ is harmonic for the metric

$$\Phi_n^*\left(dr^2 + r^2\eta d\theta^2\right) \;=\; \epsilon_n^2 e^{-2t}\left[dt^2 + \eta(\epsilon_n e^{-t}, \theta)d\theta^2\right],$$

and therefore for the metric in square brackets. The chain rule shows that $1 - \eta_n \to 0$ in C^2, and $T_n = \log(\epsilon_n/n\lambda_n) \to \infty$ by Lemma 1.3.

The first inequality in (1.19) is the usual length-energy inequality for loops parameterized by $[0, 2\pi]$. Now by definition (1.6) ϕ_n has energy at most C_R on A_n, and each point on $[1, T-1] \times S^1$ lies in a unit disk in $[0, T_n] \times S^1$, so from (1.1) it follows that

$$P_n(t) \;=\; \int_0^{2\pi} |d\phi_n|^2 \, d\theta \;\le\; 2\pi C_1 C_R \qquad \text{for } 1 \le t \le T_n - 1.$$

For $0 \le t \le 1$ and large n, $\gamma_{n,t}$ is the image under f_n of a circle that lies in the region $U_n = D(c_n, \epsilon_n) - D(c_n, \epsilon_n/8)$ to which (A.7) applies. Since $r^{-1}\partial_\theta$ becomes a unit vector as $n \to \infty$, we have

$$\sup_\theta |\partial_\theta \gamma_n(t,\theta)|^2 \;\le\; 2\sup_{U_n} r^2\,|df_n|^2 \;\le\; 4C_5\epsilon_n^2,$$

and $\epsilon_n \le 1/n$. Hence $P(t) \le 8\pi C_5/n^2 \le 2\pi C_1 C_R$ for $0 \le t \le 1$ and large n. For $T_n - 1 \le t \le T_n$, using (A.8) we get a similar bound, and the lemma follows. q.e.d.

Acknowledgement. This work was supported in part by the NSF

References

[1] H. Brezis & J.-M. Coron, *Convergence of solutions of H-systems or how to blow bubbles*, Arch. Rational Mech. Anal. **89** (1985) 21–56.

[2] J. Cheeger & D. Ebin, *Comparison theorems in Riemannian geometry*, North-Holland, Amsterdam, 1975.

[3] J. Chen & G. Tian, *Compactification of moduli space of harmonic mappings*, Preprint, 1996.

[4] H. Davis, *Introduction to nonlinear differential and integral equations*, Dover, New York, 1962.

[5] W.-Y. Ding & G. Tian, *Energy identity for a class of approximate harmonic maps from surfaces*, Comm. Anal. Geom. **4** (1995) 543-554.

[6] P. Feehan, *Geometry of the ends of the moduli space of anti-self-dual connections over negative definite four-manifolds*, J. Differential Geom. **42** (1995) 465-553.

[7] M. Grüter, *Eine Bemerkung zur regularität stationärer punkte von konform invarianten Variationsintegralen*, Manuscripta Math. **55** (1986) 451-453.

[8] F. Helein, *Régularité des applications harmoniques entre une surface at une variété Riemannienne*, C.R. Acad. Sci. Paris, Sér. I **312** (1991) 591-596.

[9] D. Hoffman & J. Spruck, *Sobolev and isoperimetric inequalities for Riemannian manifolds*, Comm. Pure Appl. Math. **27** (1974) 715-727; *Correction*, ibid. **28** (1975) 765-766.

[10] J. Jost, *Two-dimensional geometric variational problems*, Wiley, New York, 1991.

[11] C.B. Morrey, *Multiple integrals in the calculus of variations*, Springer, New York, 1966.

[12] T.H. Parker & J. Wolfson, *Pseudo-holomorpohic maps and bubble trees*, J. Geom. Anal. **3** (1993) 63-98.

[13] J. Qing & G. Tian, *Necks between bubbles*, Preprint, 1996, 543-554.

[14] R. Schoen, *Analytic aspects of the harmonic map problem*, M.S.R.I. Seminar on Nonlinear Partial Differential Equations, (ed. S.S. Chern), Springer, New York, 1984 321-358.

[15] M. Struwe, *Variational Methods, applications to nonlinear differential equations and Hamiltonian systems*, Springer, New York, 1990.

[16] J. Sacks & K. Uhlenbeck, *The existence of minimal immersions of 2-spheres*, Annals of Math. **113** (1981) 1-24.

[17] C.H. Taubes, *A framework for Morse theory for the Yang-Mills functional*, Invent. Math. **94** (1988) 337–392.

MICHIGAN STATE UNIVERSITY